Formation and Structure of Self-Assembled Monolayers

Abraham Ulman

Department of Chemical Engineering, Chemistry and Materials Science, and the Herman F. Mark Polymer Research Institute, Polytechnic University, Six MetroTech Center, Brooklyn, New York 11201

Received November 3, 1995 (Revised Manuscript Received April 18, 1996)

Contents

Abraham Ulman was born in Haifa, Israel, in 1946. He studied chemistry in the Bar-Ilan University in Ramat-Gan, Israel, and received his B.Sc. in 1969. He received his M.Sc. in phosphorus chemistry from Bar-Ilan University in 1971. After a brief period in industry, he moved to the Weizmann Institute in Rehovot, Israel, and received his Ph.D. in 1978 for work on heterosubstituted porphyrins. He then spent two years at Northwestern University in Evanston, IL, where his main interest was one-dimensional organic conductors. In 1985 he joined the Corporate Research Laboratories of Eastman Kodak Company, in Rochester, NY, where his research interests were molecular design of materials for nonlinear optics and self-assembled monolayers. In 1994 he moved to Polytechnic University where he is the Alstadt-Lord-Mark Professor of Chemistry. His interests encompass self-assembled monolayers, surface engineering, polymers at interface, and surfaces phenomena.

I. Introduction

The field of self-assembled monolayers (SAMs) has witnessed tremendous growth in synthetic sophistication and depth of characterization over the past 15 years.[1] However, it is interesting to comment on the modest beginning and on important milestones. The field really began much earlier than is now recognized. In 1946 Zisman published the preparation of a monomolecular layer by adsorption (self-assembly) of a surfactant onto a clean metal surface.[2] At that time, the potential of self-assembly was not recognized, and this publication initiated only a limited level of interest. Early work initiated in Kuhn's laboratory at Göttingen, applying many years of experience in using chlorosilane derivative to hydrophobize glass, was followed by the more recent discovery, when Nuzzo and Allara showed that SAMs of alkanethiolates on gold can be prepared by adsorption of di-*n*-alkyl disulfides from dilute solutions.[3] Getting away from the moisture-sensitive alkyl trichlorosilanes, as well as working with crystalline gold surfaces, were two important reasons for the success of these SAMs. Many self-assembly systems have since been investigated, but monolayers of alkanethiolates on gold are probably the most studied SAMs to date.

The formation of monolayers by self-assembly of surfactant molecules at surfaces is one example of the general phenomena of self-assembly. In nature, self-assembly results in supermolecular hierarchical organizations of interlocking components that provides very complex systems.[4] SAMs offer unique opportunities to increase fundamental understanding of self-organization, structure−property relationships, and interfacial phenomena. The ability to tailor both head and tail groups of the constituent molecules makes SAMs excellent systems for a more fundamental understanding of phenomena affected by competing intermolecular, molecular−substrates and molecule−solvent interactions like ordering and growth, wetting, adhesion, lubrication, and corrosion. That SAMs are well-defined and accessible makes them good model systems for studies of physical chemistry and statistical physics in two dimensions, and the crossover to three dimensions.

SAMs provide the needed design flexibility, both at the individual molecular and at the material levels, and offer a vehicle for investigation of specific interactions at interfaces, and of the effect of increasing molecular complexity on the structure and stability of two-dimensional assemblies. These studies may eventually produce the design capabilities needed for assemblies of three-dimensional structures.[5] However, this will require studies of more complex systems and the combination of what has been learned from SAMs with macromolecular science.

The exponential growth in SAM research is a demonstration of the changes chemistry as a disci-

S0009-2665(95)00235-4 CCC: $25.00

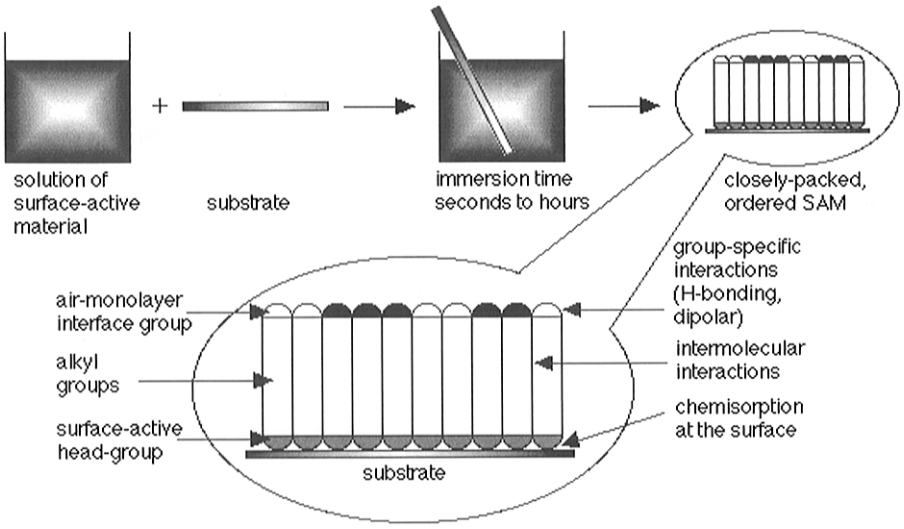

Figure 1. Self-assembled monolayers are formed by simply immersing a substrate into a solution of the surface-active material. The driving force for the spontaneous formation of the 2D assembly includes chemical bond formation of molecules with the surface and intermolecular interactions.

pline has been going through. Chemistry has been moving away from traditional disciplines and into interdisciplinary areas, and chemists are engaged in research at the interface of chemistry with physics, biology, and engineering. The fabrication and manipulations of molecular assemblies, molecular recognition, biomineralization, hierarchical structure and function, and computational chemistry to elucidate structure−function relationships have become central themes in modern chemistry. These important changes can find their origin partly in the areas of Langmuir−Blodgett and self-assembled monolayers, which continue to serve as major techniques for the fabrication of supramolecular structures.

The interest in the general area of self-assembly, and specifically in SAMs, stems partially from their perceived relevance to science and technology. In contrast to ultrathin films made by, for example, molecular beam epitaxy (MBE), and chemical vapor deposition (CVD), SAMs are highly ordered and oriented and can incorporate a wide range of groups both in the alkyl chain and at the chain termina. Therefore, a variety of surfaces with specific interactions can be produced with fine chemical control.[6] Due to their dense and stable structure, SAMs have potential applications in corrosion prevention, wear protection, and more. In addition, the biomimetic and biocompatible nature of SAMs makes their applications in chemical and biochemical sensing promising. Their high molecular order parameter in SAMs makes them ideal as components in electro-optic devices Recent work on nanopatterning of SAMs suggests that these systems may have applications in patterning of GaAs and in the preparation of sensor arrays.[7]

While the majority of papers in recent years deal with thiols on gold, this by no means is the only system to consider. Silanes on hydroxylated surfaces are important systems for many technological applications, and efforts continue to achieve better reproducibility in monolayer preparation. SAMs of fatty acid derivatives are an important link between the Langmuir−Blodgett and the self-assembly techniques and, as such, continue to be studied. In this review, we discuss structural factors in the formation of SAMs. We describe different SAMs, their unique features and provide examples of various systems. We then attempt to provide a general picture of self-assembly on surfaces, as it emerges from a consideration of the interplay of different forces that control this process.

II. Self-Assembled Monolayers

SAMs are ordered molecular assemblies formed by the adsorption of an active surfactant on a solid surface (Figure 1). This simple process makes SAMs inherently manufacturable and thus technologically attractive for building superlattices and for surface engineering. The order in these two-dimensional systems is produced by a spontaneous chemical synthesis at the interface, as the system approaches equilibrium. Although the area is not limited to long-chain molecules,[8] SAMs of functionalized long-chain hydrocarbons are most frequently used as building blocks of supermolecular structures.

1. Monolayers of Fatty Acids

Spontaneous adsorption of long-chain *n*-alkanoic acids ($C_nH_{2n+1}COOH$) has been studied in the past few years. This is an acid−base reaction, and the driving force is the formation of a surface salt between the carboxylate anion and a surface metal cation. Allara and Nuzzo[9,10] and Ogawa *et al.*[11] studied the adsorption of *n*-alkanoic acids on aluminum oxide. Schlotter *et al.* studied the spontaneous adsorption of such acids on silver.[12] Huang and Tao studied SAMs of long-chain diacetylene amphiphiles.[13] In this rigid, rodlike systems, the diacetylene π-system breaks the cylindrical symmetry of the *all-trans*-alkyl chain. Thus, if one views the two-dimensional packing of fatty acids as a close-packed assembly of ordered *all-trans*-alkyl chains, the diacetylene units introduce a stratum of defects into this assembly.[14] As a result, the highest contact angle was recorded on a monolayer where the diacetylene group is connected to the carboxylic head group, i.e., the stratum of defects is as far as possible from the air−monolayer interface, so that high ordering and close-

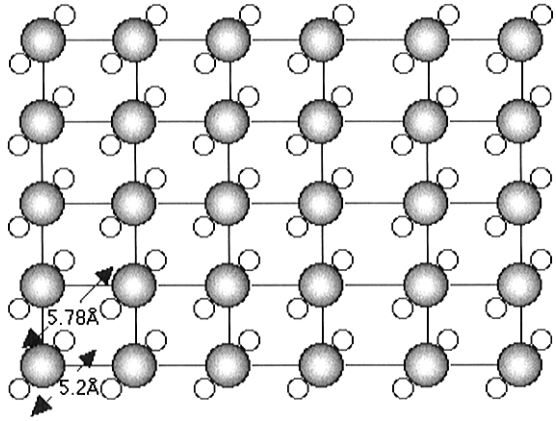

Figure 2. The p(2×2) adsorption scheme of fatty acids on AgO. The filled circles are the carboxylate carbon atoms, while the small, hollow circles are carboxylate oxygen atoms.

packing can be restored. Grazing incidence X-ray diffraction (GIXD) of docosanoic acid ($CH_3(CH_2)_{20}$-COOH) monolayers on AgO reveals that the carboxylate anion adsorbs in a p(2×2) overlayer structure, with a lattice spacing of 5.78 Å (Figure 2).[15] The alkyl chains are in *all-trans* extended configuration, and are tilted 26.7° from the surface normal. The plane that bisects the methylene groups is twisted with respect to the plane of the carboxylate group. Polarized infrared external reflection spectroscopy (PIERS) studies confirm this structure.[12,16] Studies show that the structures of monolayers formed from solution and from the gas phase on AgO are identical.[17]

Tao showed that the chemisorption of alkanoic acids on amorphous metal oxide surfaces is not unique.[16] It was found that on AgO surfaces, the carboxylate two oxygen atoms bind to the surface nearly symmetrically, while on surfaces of CuO and Al_2O_3, the carboxylate binds asymmetrically to the surface displaying tilt angles close to zero (Figure 3). Recent Raman studies suggest that a monolayer of stearic acid adsorbed to a smooth Ag surface is less ordered that the stearic acid layer on Al_2O_3[17] and that the chain in SAMs on AgO are oriented along the surface normal, confirming previous observations by Allara and Nuzzo,[9,10] Smith and Porter,[18] and Soundag *et al.*[19] However, infrared studies by Tao suggest that monolayers on AgO are more ordered than their counterparts on Al_2O_3.

Differences between results in two groups are not uncommon in this area of research, and may result from differences in preparation protocols. Clearly more work needs to be done to resolve these differences. In a later study, Tao *et al.* investigated the self-assembly of biphenyl- and naphthyl-containing alkanoic acids.[20] They demonstrated that biphenyl or naphthyl groups, due to their larger cross sectional area, cause higher tilt of molecular chains in carboxylic acid monolayers on silver and a correlation of wetting properties and chain tilt. Different behavior observed on silver and copper has been attributed to site specificity, binding geometry, and binding strength, among other factors.

2. Monolayers of Organosilicon Derivatives

SAMs of alkylchlorosilanes, alkylalkoxysilanes, and alkylaminosilanes require hydroxylated surfaces as substrates for their formation. The driving force for this self-assembly is the in situ formation of polysiloxane, which is connected to surface silanol groups (−SiOH) via Si−O−Si bonds. Substrates on which these monolayers have been successfully prepared include silicon oxide,[21−26] aluminum oxide,[27,28] quartz,[29−31] glass,[26] mica,[32−34] zinc selenide,[26,27] germanium oxide,[26] and gold.[35−37] Recently Allara *et al.* have compared OTS monolayers on silicon oxide and on gold activated by UV−ozone exposure. IR spectroscopy, ellipsometry, and wetting measurements showed identical average film structures.[38]

High-quality SAMs of alkyltrichlorosilane derivatives are not simple to produce, mainly because of the need to carefully control the amount of water in solution.[22,39,40] While incomplete monolayers are formed in the absence of water,[23,24] excess water results in facile polymerization in solution and polysiloxane deposition of the surface.[29] Recently, McGovern *et al.* have shown that extraction of surface moisture, followed by OTS hydrolysis and subsequent surface adsorption may be the mechanism of SAM formation.[41] They suggested a moisture quantity of 0.15 mg/100 mL of solvent as the optimum condition for the formation of closely packed monolayers. X-ray photoelectron spectroscopy (XPS) studies confirm the complete surface reaction of the $-SiCl_3$ groups, upon the formation of a complete SAM.[42] Recently, Tripp and Hair used infrared spectroscopy to provide direct evidence for the full hydrolysis of methylchlorosilanes to methylsilanols, at the solid−gas interface, by surface water on a hydrated silica.[43]

Temperature has been found to play an important role in monolayer formation. The threshold temperature below which an ordered monolayer is formed was found to be a function of the chain length (higher for octadecyl−18 °C−than for tetradecyl chain−10 °C).[22] Here, the issue is the competition between the reaction of hydrolyzed (or partially hydrolyzed) trichlorosilyl groups with other such groups in solution to form a polymer, and the reaction of such groups with surface Si−OH moieties to form a SAM. As temperature decreases, the preference of surface reaction increases. Moreover, as temperature decreases, reaction kinetics decreases as well, resulting in the diminution on of thermal disorder in the forming monolayer, the formation of an ordered assembly, and the gain of van der Waals (VDW) energy. Recent solid-state ^{13}C NMR studies of OTS monolayers deposited on fumed silica particles confirm these results.[44]

Since substrates used in the formation of silane SAMs are amorphous, the packing and ordering of alkyl chains in SAMs of alkyl silanes are determined by the underlying structure of the surface polysiloxane chain. A schematic description of a polysiloxane at the monolayer substrate interface is shown in Figure 4. The dotted line on the left is a bond in a possible precursor trimer (see dashed frame in Figure 4), where the alkyl chains can occupy either axial or equatorial positions.[1] In this trimer, siloxane oxygens occupy the equatorial positions and the alkyl chains are connected to the axial positions, with interchain distance of ∼4.4 Å. This leaves very little free volume and should require very little or no chain tilt. The connection between free volume and tilt is

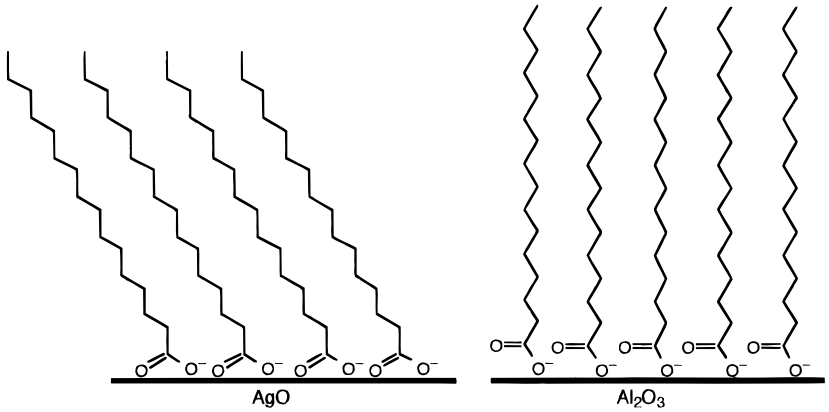

Figure 3. A schematic description of fatty acid monolayers on Ago and on Al_2O_3.

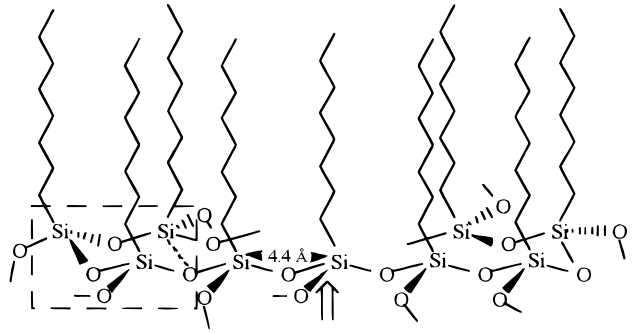

Figure 4. A schematic description of a polysiloxane at the monolayer−substrate surface. The arrow points to an equatorial Si−O bond that can be connected either to another polysiloxane chain or to the surface. (Adapted from Ulman, A., ref 1. Copyright 1991 Academic Press.) The dotted line on the left is a bond in a possible precursor trimer.

a general one, since the driving force for tilt is the reestablishment of VDW contact among chains.

Allara *et al.* found that alkyl chains in OTS monolayers of SiO_2 and oxidized gold are tilted at 10 ± 2° from the normal, with significant *gauche* defect content at the chain termina.[38] On the basis of both ellipsometry and the concentration of *gauche* defects, it was concluded that the monolayer is ∼96 ± 4% of the theoretical maximum coverage, which explains the observed average tilt. An important conclusion of this study is that surface hydration is responsible for decoupling of film formation from surface chemistry and the observed high film quality. Increasing surface attachment of the forming siloxane chain, through surface Si−OH groups, introduces disorder and film defects.

Biernbaum *et al.* used near-edge X-ray absorption fine structure spectroscopy (NEXAFS) and X-ray photoelectron spectroscopy (XPS) to study SAMs of OTS, octadecyltrimethoxysilane [OTMS, $CH_3(CH_2)_{17}Si(OCH_3)_3$], and (17-aminoheptadecyl)trimethoxysilane [AHTMS, $H_2N(CH_2)_{17}Si(OCH_3)_3$].[45] A number of important observations have been reported. First, that the chains in OTS SAMs are practically perpendicular to the substrate surface (tilt angle 0 ± 5°). Second, that the adsorption mechanisms of trichlorosilane and trimethoxysilane groups are different, resulting in a higher tilt angle of the chains in OTMS SAMs (20 ± 5°). Third, that the introduction of a polar amino group at the chain termina results in a more disordered monolayer, probably as a result of acid−base interactions with surface silanol groups. This observation suggests that when such interactions exist, a preferred route may be to create surface functionalities by chemical reactions.

The reproducibility of alkyltrichlorosilane monolayers is still a problem, since the quality of the monolayer formed is very sensitive to reaction conditions. For example, Silberzan *et al.* reported that 3 min is enough for the formation of a monolayer,[22] while Wasserman *et al.* suggested over 24 h,[23] and Banga *et al.* 90 min.[46] Sagiv reported that hexadecane is not incorporated in OTS monolayers,[25] while Tripp and Hair reported the opposite.[39] Cohen and Sagiv suggested that partial OTS monolayers have heterogeneous island structure,[25,47] while Ohtake *et al.*,[48] Mathauser and Frank,[30,31] Wasserman and co-workers,[42,49] and Ulman[1] concluded that these incomplete monolayers are homogeneous and disorder. In fact, Wasserman *et al.* did not carry out off-specular reflection measurements, which is why they could not detect the island structure. Recent AFM studies have confirmed the island structure of partial monolayers. Banga *et al.* studied the adsorption of OTS onto glass and silicon oxide surfaces,[46] and Israelachvili and co-workers investigated the adsorption of OTS on mica.[34] They discovered that OTS forms monolayers on mica by nucleating isolated domains, whose fractal dimensions increase with increased surface coverage. Other AFM images of OTS SAMs on mica and on silica and silicon have also been produced.[50−57] Nakagawa *et al.* showed that there were pin holes in the OTS films from several nanometers to 100 nm in diameter, in monolayers on mica formed by self-assembly from a solvent mixture.[50] Grunze *et al.* Studied OTS SAMs on silicon and emphasized that in order to obtain reproducible, good quality films, samples must be prepared under class 100 clean room conditions.[54] They found that OTS SAMs formed on silicon, first by growth of large island and then by filling in with smaller islands until the film is complete. (Mathauer and Frank utilized this growth mechanism to form binary SAMs of OTS and 11-(2-naphthyl)undecyltrichlorosilane.[58]) Other researchers suggested that in partial (25−30%) monolayers OTS molecules lie flat on the silicon surface, producing a water contact angle of 90°.[55]

Differences in reported results also exist for other alkyltrichlorosilane systems. Netzer *et al.* reported that surface coverages of vinyl-terminated alkyltrichlorosilane were only ∼63%,[59] while Silberzan

and Léger obtained well-packed monolayers using the same silane derivatives.[22] Pomerantz *et al.* stated that surface coverage for monolayers of methyl 23-(trichlorosilyl)tricosanoate ($H_3CO_2C(CH_2)_{22}SiCl_3$, MTST) is ~93%,[60] while Tillman prepared full monolayers using the same molecule.[61]

Patterns of ordered molecular islands surrounded by disordered molecules are common in Langmuir layers, where even in zero surface pressure molecules self-organize at the air−water interface. The difference between the two systems is that in SAMs of trichlorosilanes the islands comprise of polymerized surfactants, and therefore the mobility of individual molecules is restricted. This lack of mobility is probably the major reason why SAMs of alkyltrichlorosilanes are less ordered than, for example, fatty acids on AgO, or thiols on gold. The coupling of polymerization and surface anchoring is a major source of the reproducibility problems discussed above. This is because small differences in water content and in surface Si−OH group concentration may result in significant difference in monolayer quality. Notwithstanding, due to the unique stability of their complete monolayers, alkyl silanes are ideal materials for surface modification and functionalization applications, for example, as adhesion promoters,[62−64] and boundary lubricants.[65−67]

Surface modification can be achieved either by using ω-substituted alkyl silanes, or by surface chemical reactions. SAMs have been reported from alkyltrichlorosilanes with terminal functional groups of halogen,[68−72] cyanide,[69] thiocyanide,[69] methyl ether,[68] acetate,[68] thioacetate,[68,73] α-haloacetate,[70] vinyl,[22,23,59,74−80] (trimethylsilyl)ethynyl,[81] methyl ester,[60,61] and *p*-chloromethylphenyl.[70,82−85] Monolayers with low surface free energy have been prepared using partially fluorinated alkylsilanes.[49,68,86,87] Surface modification can also be performed using various nucleophilic substitution on SAMs of 16-bromohexadecylsilane.[69] Thus, the aforementioned SAMs were converted to the 16-thiocyanatohexadecylsilane monolayers by simply treating them with a 0.1 M KSCN solution in DMF for 20 h. Similarly, NaN_3, Na_2S, and Na_2S_2 gave complete conversions of the bromo-terminated monolayers, as was evident from X-ray photoelectron spectroscopy (XPS).[69] Reduction of the thiocyanato, cyanide, and azide surfaces by $LiAlH_4$ gave the mercapto- and amino-terminated monolayers in complete conversions.[69] Oxidation of the ω-thiol group gave sulfonic acid surfaces.[69] XPS investigations of nucleophilic substitution at chain termina of alkyltrichlorosilane monolayers, using *p*-nitrothiophenolate as the nucleophile, were carried out by Sukenik and co-workers.[70] They report that reaction rates obey the following order of leaving groups I > Br > Cl, and $XCH_2CO > PhCH_2X > CH_2$-CH_2X. Competition reactions using thiolates and amines as nucleophiles show a clear thiolate preference. Reactions with small peptide fragments with cysteine moieties as the nucleophiles resulted in grafting of the monolayer surface with these peptides. This may be important for the development of biosensors. Recently reported patterned SAMs formed by microcontact printing of alkyltrichlorosilane on Al_2O_3/Al, SiO_2/Si, and TiO_2/Ti, while focused on selective CVD of metals by inhibiting nucleation, open new opportunities for preparation of sensors and electrooptical devices.[88,89]

Surface modification reactions are important not only for engineering of surface energy and interfacial properties such as wetting, adhesion, and friction, but also for providing active surfaces for the attachment of molecules with different properties. For example, the reaction of bromo-terminated alkylsilane monolayers with the lithium salt of 4-methylpyridine to provide pyridine surfaces.[71,72] Such surfaces react with palladium,[90] rhenium,[72] and osmium complexes[71] and provide immobilization of organometallic moieties. Interestingly, immobilized OsO_4 reacts with C_{60} Bucky balls, resulting in the formation of a C_{60} monolayer.[71] Similar monolayers can be formed by the reaction of Bucky balls with amino or azido surface groups.[91−93] Cystein-specific surface was prepared by Bohm *et al.* for the fabrication of metalloprotein nanostructures.[94] These examples show the opportunities SAMs provide in the construction of layers and of new materials by combinations thereof.

Mixed monolayers provide an excellent route for surface engineering at the molecular level. Hence, by coadsorption of alkyltrichlorosilane with different ω-functionalities, surface free energy and chemical reactivity can be designed via the control of surface chemical functionalities. However, there are few reports on mixed monolayers of alkyltrichlorosilane, and most investigations were carried out on alkanethiolate monolayers on gold. When mixed monolayers of alkyltrichlorosilane and (ω-vinylalkyl)- or [ω-(2-naphthyl)alkyl]trichlorosilane were prepared by competitive adsorption, it was found that the composition of the monolayer is equal to the composition of the immersion solution.[23,24,30] The gradual increase of the amount of excimers observed with the gradual increase of the naphthyl concentration supports the ideal mixing of the two silanes in the monolayer. When the preparation of mixed monolayers of alkyltrichlorosilanes with different chain length was investigated, ideal mixing was also observed, with the composition being determined by the relative rates of adsorption of the components.[95]

Construction of multilayers requires that the monolayer surface be modified to a hydroxylated one. Such surfaces can be prepared by a chemical reaction and the conversion of a nonpolar terminal group to a hydroxyl group. Examples of such reactions are the $LiAlH_4$ reduction of a surface ester group,[61] the hydroboration−oxidation of a terminal vinyl group,[23,59] and the conversion of a surface bromide using silver chemistry.[96] Once a subsequent monolayer is adsorbed on the "activated" monolayer, multilayer films may be built by repetition of this process (Figure 5).

Using this strategy, Tillman *et al.* demonstrated the construction of multilayer films of ~0.1 μm thickness by self-assembly of MTST on silicon substrates (Figure 6).[61] The linear relationship between the film thickness and the layer number showed a slope of 35 Å/layer. Ellipsometry data, absorbance intensities, and dichroic ratios for the multilayers all suggested that the samples were composed of distinct monolayers. However, IR data indicated that there may be more tilting or disordering of the alkyl chains

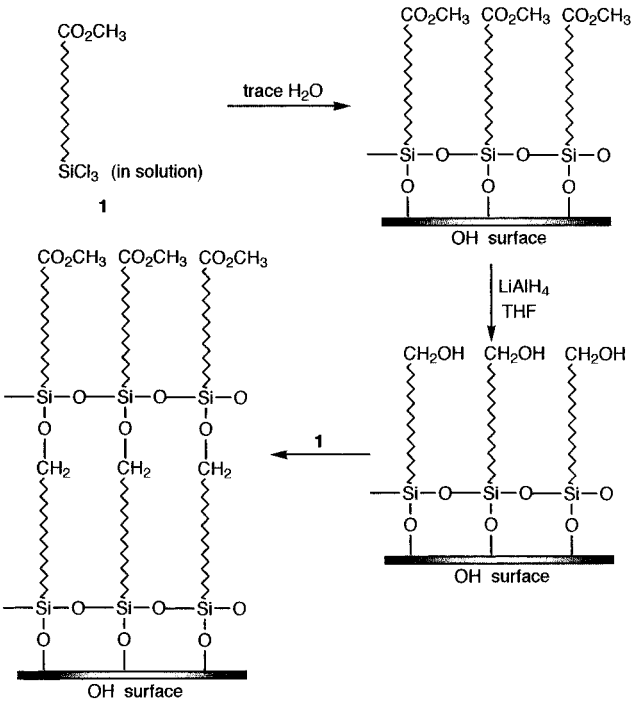

Figure 5. Construction of self-assembled multilayers from methyl 23-(trichlorosilyl)tricosanoate.

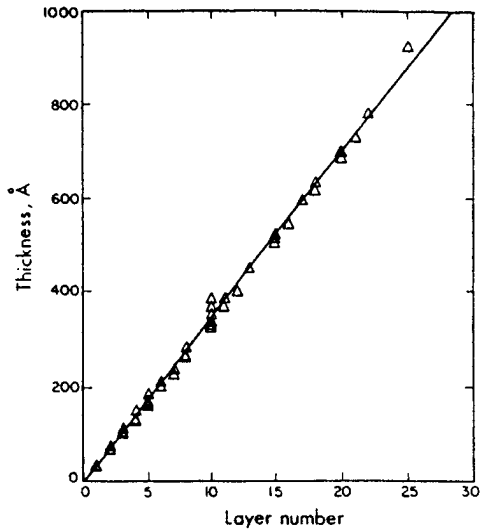

Figure 6. Film thickness vs layer number. (From Tillman et al., ref 61. Copyright 1988 American Chemical Society.)

in the seven-layer sample than for the monolayer samples.

Despite the increasing level of monolayer disorder, the preparation of a multilayer film with thickness of ~0.1 mm was possible. Therefore, it is likely that the in situ formation of a polysiloxane backbone at the substrate−solution interface allows the monolayer to "bridge over" defects, such as pinholes and unreduced carbonyl groups. This repair mechanism may be very significant, because it is difficult to imagine the construction of very thick films (1−2 μm, 250−500 layers) by self-assembly, if defects inevitably propagate and grow.

Synchrotron X-ray diffraction studies were performed on a 15-layer thin film of MTST.[97] The specular profile suggested a compression of the outmost layers from an average spacing of 31.90 ± 0.02 Å, which is interpreted as an increase in disordering near the film/air interface. Rocking curves of the specular profile suggest extremely rigid $-SiO_2-$ layers. In-plane results also depict rigid $-SiO_2-$ layers, with ad-spacing of 1.35 ± 0.03 Å, with an increase in disorder at below critical angle measurements. The alkyl chains were shown to be hexagonally packed between these rigid layers, and there was no observance of a chain tilt.

Marks and co-workers have developed a self-assembly strategy, where the $-SiCl_3$ group is attached to a small molecules and an S_N2 reaction with the SAM introduced a monolayer of NLO-active dyes. Thus, SAMs of [2-(*p*-chloromethylphenyl)ethynyl]-silane react with [2-[4-[*N*,*N*-bis(3-hydroxypropyl)-amino]phenyl]ethynyl]-4′-pyridine. The latter was used in the construction of SAMs with second-harmonic nonlinear optical (NLO) properties.[81−85] A major improvement in the synthesis of multilayer structure has been reported recently by Marks *et al.* They found that spin coating of a dilute solution of [[4-[*N*,*N*-bis(3-hydroxypropyl)amino]phenyl]azo]-4′-pyridine on a benzyl chloride SAM surface, followed by annealing at 110°, results in the facile formation of SAMs, with high order parameter (Figure 7).

Using this process they could prepare a three-layer system in 1 h (Figure 7).[98] While it is still not a fast enough process for the construction of electrooptic devices, the combination of SAM with spin coating is a step forward in the development of SAM-based thin-film applications.

Sagiv *et al.* have reported hydrogen-bonded multilayers of self-assembling silanes.[99,100] Using a combination of FTIR spectroscopy and X-ray scattering they describe the multilayer structure as district monolayers, coupled to each other in a flexible, nonepitaxial manner, via interlayer multiple hydrogen bonds. The hydrocarbon chains are perpendicular to the layer plane, with a lateral packing density of 21 Å per molecule and a positional coherence length of ca. 70 Å. However, the authors do not provide experimental details, and no corroborative data from other groups is available.

Ogawa showed that [19-(trimethylsilyl)-18-nonadecynyl]silane monolayers can be polymerized to the corresponding polyacetylene systems.[81] The treatment of the nonpolymerized monolayers with electron beam radiation is dependent on ambient conditions. When irradiation was carried out under helium, the result was cross-linked monolayers; however, when irradiation was done under nitrogen, cross-linking was accompanied by the formation of amino terminal groups, and when it was carried out under oxygen, cross-linked monolayers with hydroxy, aldehyde, and carboxylic acid terminal groups were obtained. By using this technique, it was possible to fabricate multilayer films,[80] but, with nonlinear relationship between film thickness and the number of layers.[101] Attempts to prepare thicker films failed due to increased disorder. It appears that there is competition between irradiation damage and the formation of a new layer.[102]

While there has been a considerable hope that SAMs of silane derivatives can be used to form nonlinear optical devices such as wave guides, where angstrom-level control of film thickness and therefore phase matching are possible, there has been no demonstration of success yet. This is primarily the

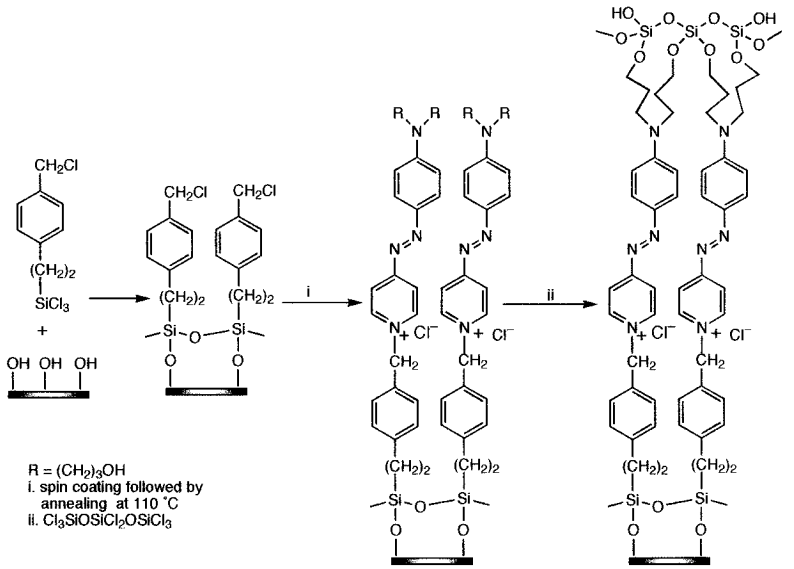

Figure 7. Formation of noncentrosymmetric multilayer film by combining self-assembly and a surface S_N2 reaction.

result of serious drawbacks of both materials and process issues. Trichlorosilane derivatives of large dye molecules are difficult to purify and due to their moisture sensitivity hard to handle. Their organic solutions tend to become turbid rather quickly due to the formation of insoluble polymers in solution. Thus, in a real process, solutions must be replaced frequently. Therefore, it is unrealistic to suggest utilizing trichlorosilane derivatives for the formation of self-assembled multilayers. One exception may be the combination of self-assembly and surface chemical reaction as demonstrated by Marks' group,[82−85,98] especially if conditions are further developed to expedite monolayer formation. On the other hand, ω-substituted alkyltrichlorosilane derivatives—easy to synthesize and purify materials—can be used for the engineering of surface free energy through the control of chemical functionalities in their SAMs, or as active layers for attachment of biomolecules in biosensors.

3. Organosulfur Adsorbates on Metal and Semiconductor Surfaces

Sulfur and selenium compounds have a strong affinity to transition metal surfaces.[103−107] This is probably because of the possibility to form multiple bonds with surface metal clusters.[108] The number of reported surface active organosulfur compounds that form monolayers on gold has increased in recent years (Figure 8). These include, among others, di-*n*-alkyl sulfide,[109,110] di-*n*-alkyl disulfides,[3] thiophenols,[111,112] mercaptopyridines,[112] mercaptoanilines,[113] thiophenes,[114] cysteines,[115,116] xanthates,[117] thiocarbaminates,[118] thiocarbamates,[119] thioureas,[120] mercaptoimidazoles,[121−123] and alkaneselenols.[124] However, the most studied, and probably most understood SAM is that of alkanethiolates on Au(111) surfaces.

It was suggested that gold does not have a stable surface oxide;[125] therefore, its surface can be cleaned simply by removing the physically and chemically adsorbed contaminants. However, recently King showed that oxidation of gold by UV and ozone at 25 °C gives a 17 ± 4 Å thick Au_2O_3 layer,[126] which was stable to extended exposure to ultrahigh vacuum (UHV) and water and ethanol rinses.

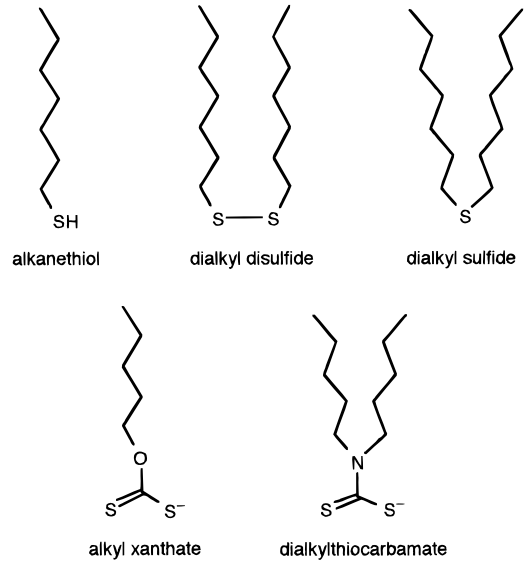

Figure 8. Surface-active organosulfur compounds that form monolayers on gold.

Organosulfur compounds coordinate very strongly also to silver,[127−131] copper,[129−132] platinum,[133] mercury,[134,135] iron,[136,137] nanosize γ-Fe_2O_3 particles,[138] colloidal gold particles,[139] GaAs,[140] and InP surfaces.[141] However, most investigations have been carried out on SAMs of thiolates on Au(111) surfaces. Interestingly, octadecanethiol monolayers provide an excellent protection of the metal surface against oxidation.[132] For example, silver surfaces with octadecanethiolate monolayers could be kept in ambient conditions without tarnishing for many months, and copper surfaces coated with the same monolayer sustain nitric acid.[142]

Kinetic studies of alkanethiol adsorption onto Au(111) surfaces have shown that at relatively dilute solutions (10^{-3} M), two distinct adsorption kinetics can be observed: a very fast step, which takes a few minutes, by the end of which the contact angles are close to their limiting values and the thickness about 80−90% of its maximum, and a slow step, which lasts several hours, at the end of which the thickness and contact angles reach their final values.[143] The initial step—described well by diffusion-controlled Langmuir

adsorption—was found to strongly depend on thiol concentration. At 1 mM solution the first step was over after ~1 min, while it required over 100 min at 1 μM concentration.[143] The second step can be described as a surface crystallization process, where alkyl chains get out of the disordered state and into unit cells, thus forming a two-dimensional crystal. Therefore, the kinetics of the first step is governed by the surface—head group reaction, and the activation energy may depend on the electron density of the adsorbing sulfur. On the other hand, the kinetics of the second step is related to chain disorder (e.g., gauche defects), the different components of chain—chain interaction (VDW, dipole—dipole, etc.), and the surface mobility of chains. It also was found that the kinetics is faster for longer alkyl chains, probably due to the increased VDW interactions.[143]

Second-harmonic generation, and XPS measurements,[144,145]as well as near edge X-ray absorption fine structure (NEXAFS) studies confirmed the two-step mechanism.[146] Studies also showed pronounced differences between the short ($n < 9$) and long ($n > 9$) alkanethiolates. This is probably due to the decreased rate of the second step resulting from the diminution of the interchain VDW attraction energy. In the case of simple alkyl chains, the masking of adsorption sites by disordered chains is not a serious problem. However, if the chain contains a bulky group, the two steps are coupled, and the chemisorption kinetics is greatly impeded by the chain disorder.[147] A direct competition between *tert* -butyl mercaptan and *n*-octadecyl mercaptan reveals that the latter adsorbed onto gold with greater efficiency that the former by a factor of 290—710 from ethanol.[148] The additive effects of the stabilizing van der Waals interactions in the *n*-alkyl mercaptan monolayer and the sterically hindered *tert*-butyl mercaptan explain the clear preference of the linear molecules.

Chemisorption of alkanethiols as well as of di-*n*-alkyl disulfides on clean gold gives indistinguishable monolayers,[149] probably forming the Au(I) thiolate (RS^-) species. A simple oxidative addition of the S—S bond to the gold surface is possibly the mechanism in the formation of SAMs from disulfides:

$$RS{-}SR + Au_n^0 \rightleftharpoons RS^-Au^+ \cdot Au_n^0$$

The rates of formation of SAMs from dialkyl disulfides or alkanethiols were indistinguishable, but the rate of replacement of molecules from SAMs by thiols were much faster than by disulfides.[149] Reaction of an unsymmetrical disulfide ($HO(CH_2)_{10}SS(CH_2)_{10}CF_3$) with a gold surface gave SAMs containing equal proportions of the two thiolate groups.[150] Replacement experiments showed that the $S(CH_2)_{10}CF_3$ group in the mixed SAMs is replaced by $S(CH_2)_{10}CN$ on exposure to the $HS(CH_2)_{10}CN$ solution in ethanol about 10^3 times faster than the $HS(CH_2)_{10}OH$ group. This is a strong support of the disulfide bond cleavage mechanism and the subsequent formation of gold thiolate species. Interestingly, Mohri *et al.* reported recently that 4-aminobenzenethiol is spontaneously oxidized to 4,4′-diaminodiphenyl disulfide in the presence of gold powder, the first observation of its kind.[151] This result hints that the stability of thiolate SAMs on gold may be related to the electron density on the thiolate sulfur. However, except for the report of Fenter *et al.* on the dimerization of alkanethiolates of Au(111) surface to form the dialkyl disulfides,[152] there has been no other *direct* evidence supporting such a reaction.

In the alkanethiole case, the reaction may be considered formally as an oxidative addition of the S—H bond to the gold surface, followed by a reductive elimination of the hydrogen. When a clean gold surface is used, the proton probably ends as a H_2 molecule. This can be deduced from the fact that monolayers can be formed from gas phase,[139,153,154] in the complete absence of oxygen:

$$R{-}S{-}H + Au_n^0 \rightleftharpoons R{-}S^-Au^+ \cdot Au_n^0 + {}^1/_2H_2$$

The combination of hydrogen atoms at the metal surface to yield H_2 molecules may be an important exothermic step in the overall chemisorption energetics. That the adsorbing species is the thiolate (RS^-) has been shown by XPS,[129,155—157] Fourier transform infrared (FTIR) spectroscopy,[158] Fourier transform mass spectrometry,[159] electrochemistry,[160] and Raman spectroscopy.[161—163] The bonding of the thiolate group to the gold surface is very strong (homolytic bond strength is approximately 40 kcal mol^{-1} [103]).

On the basis of the bond energies of RS—H, H_2, and RS—Au (87, 104, and 40 kcal mol^{-1}, respectively), the net energy for adsorption of alkanethiolates on gold would be *ca.* −5 kcal mol^{-1} (exothermic). A value of −5.5 kcal mol^{-1} has been calculated by Schlenoff using electrochemical data,[164] suggesting that the estimate of 40 kcal mol^{-1} for the S—Au bond strength is probably correct. On the basis of the similar calculations the value of *ca.* −24 kcal mol^{-1} was estimated for the adsorption energy of dialkyl disulfide, or −12 kcal mol^{-1} per RS^-, about twice as favorable as the adsorption energy calculated for the thiol mechanism involving molecular hydrogen.[164] In view of Fenter *et al.* disulfide picture,[152] Schlenoff *et al.* applied desorption data to first-order kinetics and reported better correlation in this case than for the second-order kinetics mechanism.[164] This, however, cannot be considered as direct evidence for thiolate dimerization. With all that in mind, it is not clear why a dialkyl disulfide molecule will remain adsorbed as such, with *gauche* defects at the S—C bonds to allow the hydrocarbon chains to assume hexagonal close-packing, if it can simply adsorb as two *all-trans*-alkanethiolates.

The incomplete stability of alkanethiolate SAMs can be concluded for a number of papers, although until recently there has been no conclusive evidence. Hickman *et al.* reported some loss in electroactivity of ferrocenyl alkanethiolate SAMs upon soaking in hexane,[165] while Collard and Fox did not observed such loss when the same SAM was immersed in ethanol.[166] Exposure of other electroactive SAMs to nonaqueous electrolytes also gave clues of instability.[167—169] Recently alkanethiolates bearing radiolabeled (^{35}S) head groups have been incorporated into SAMs on a variety of substrates.[164] This work addresses issues that are central to our understanding of thiolate SAMs. The question of S—C bond cleavage during adsorption to yield adsorbed sulfide (S^{2-}) and thiolate (SH^-) has been raised after Zhong and Porter reported S—C cleavage in organosulfides (R—S—R) on adsorption to gold, producing SAMs

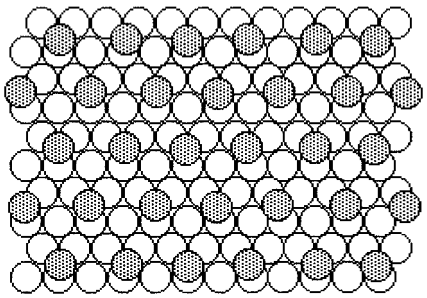

Figure 9. Hexagonal coverage scheme for alkanethiolates on Au(111). The open circles are gold atoms and the shaded circles are sulfur atoms.

identical to those resulting from S−H breaking in the corresponding thiol or from S−S breaking in the corresponding disulfides.[170] On the basis of coverage measurements Schlenoff *et al.* conclude that if any C−S bond cleavage occurs it is minimal.[164]

The thermal stability of alkanethiolate SAMs has been addressed in a number of papers. Nuzzo *et al.* have reported loss of sulfur from hexadecanethiolate monolayer on gold over the range of 170−230 °C.[165] They also performed temperature-programmed desorption of methanethiolate SAMs on gold and reported a desorption maximum at ∼220 °C.[158] Jaffey and Madix performed detailed mass spectroscopic studies of 2-methylpropanethiolate monolayers on gold and reported maximum desorption at ∼200 °C.[171] By using radiolabeled hexadecanethiolate monolayers, a complete loss of surface sulfur at 210 °C was observed with some loss occurring at 100 °C.[164]

Early electron diffraction studies (both high[172,173] and low energy[174]) of monolayers of alkanethiolates on Au(111) surfaces show that the symmetry of sulfur atoms is hexagonal with an S···S spacing of 4.97 Å, and calculated area per molecule of 21.4 Å^2. Helium diffraction[175] and atomic force microscopy (AFM)[176] studies confirmed that the structure formed by docosanethiol on Au(111) is commensurate with the underlying gold lattice and is a simple $\sqrt{3}\times\sqrt{3}$R 30° overlayer (Figure 9). However, recent ultrahigh vacuum STM studies added important information on the mechanism of SAM formation. It revealed the coexistence of a two-dimensional (2D) liquid phase at room temperature of butanethiolate ($CH_3(CH_2)_3S^-$) and hexanethiolate ($CH_3(CH_2)_5S^-$) monolayers on Au(111).[177] No 2D liquid was observed for octanethiolate ($CH_3(CH_2)_7S^-$) and decanethiolate ($CH_3(CH_2)_9S^-$) monolayers. The short-chain homologues exhibited slow desorption of surface thiolate that led to the nucleation and growth of ordered domains having a unit cell of $p\times\sqrt{3}$ ($8 \le p \le 10$). On the other hand, both octane- and decanethiolate form densely packed SAMs with a c(4×2) superlattice of a $\sqrt{3}\times\sqrt{3}$R30° lattice.[178−180]

The above STM study also discovered a facile transport of surface gold atoms in the presence of the liquid phase. This suggests that the two-step mechanism does not provide a complete picture of the surface reactions, and that adsorption/desorption processes may have an important role in the formation of the final equilibrium structure of the monolayer. Support for the importance of a desorption process comes from atomic absorption studies showing the existence of gold in the alkanethiol solution. STM studies suggest that this gold comes from terraces, where single atomic deep pits are formed.[180−182]

Ab initio calculations show that at the hollow site of Au(111), the sulfur charge is *ca.* −0.4e,[108] whereas at the on-top site, this charge is *ca.* −0.7e.[108] Since S−H bond cleavage occurs at the on-top site,[183] if this cleavage is the rate-determining step, the adsorption rate should be faster in polar solvents, due to the stabilization of the forming dipole. However, if the migration of a thiolate from the on-top to the hollow site is the slow step, the reaction should be faster in nonpolar solvent, due to the diminished charge separation. Recent second-harmonic generation studies showed that while the rate constant in ethanol is 1.3×106 cm^3 mol^{-1} s^{-1}, it is 4.7×106 cm^3 mol^{-1} s^{-1} in hexane,[184] suggesting that S−H bond cleavage is not the rate-determining step.

Migration of thiolates between neighboring hollow sites is essential for healing of defects. Such migration should occur either through the on-top or the bridge sites. In both cases, the transition state is more polar than the ground state, and hence should be sensitive to dielectric constant. Indeed, ethanol has been found to yield consistently highly ordered monolayers.[143] Notice that the thiolate is chemically bonded to one gold atom at the on-top site, forming a neutral gold thiolate molecule (RS−Au). This may desorb before the thiolate moves to the hollow site, thus leaving a defect. Recent STM studies suggest that some of the pinholes observed in monolayers on Au(111) may be a result of such an etching process.[182] However, it is also possible that alkanethiolates desorb from the surface as $RS^-Au_3^+$. These pinholes disappeared after annealing the monolayers at 77 or 100 °C,[185,186] If alkanethiolates increase the mobility of gold atoms at the surface is not clear, however, the data so far indicates that surface migration of gold thiolate molecules (RS−Au) may be considered as a possible mechanism for healing monolayer defects.

Alkanethiolates have two binding modes at the Au(111) hollow site, one with a bend angle around the sulfur of 180° (sp) and the other of 104° (sp^3), the latter being more stable by 0.41 kcal mol^{-1}.[108] Thus, packing requirements may dictate the final surface−S−C angle. Many studies have suggested that this angle in monolayers on Au(111) surfaces must be tetrahedral.[159] Modeling of terphenylthiolate ($C_6H_5-C_6H_4-C_6H_4-S-$) monolayers on Au(111) suggest a tilt angle of ∼6° from the surface normal,[111] and preliminary X-ray diffraction studies of 4-methyl-4′-mercaptobiphenyl monolayers on Au(111) single crystal surfaces confirm this suggestion,[187] thus providing the first evidence that a second chemisorption mode is possible.

The energy barrier between the two chemisorption modes on Au(111) is very small (2.5 kcal mol^{-1}),[108] suggesting that the thiolate may easily cross from one of these minima to the other, thus enabling a facile annealing mechanism (Figure 10). This predicts that the process of changing tilt direction may occur well below the melting point of the monolayer, and should be chain length dependent.

Recent X-ray data show narrowing of the diffraction peak when monolayers of alkanethiolates on

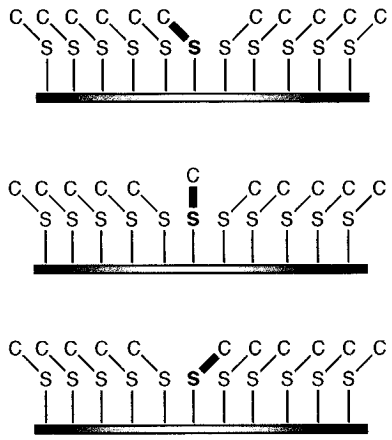

Figure 10. A possible scenario for annealing of alkanethiolate monolayers. The hybridization change results in the motion of only one chain. The arrow represents the grain boundary. Notice that after the molecule has moved, the grain boundary moved from the right of, to the left of, that molecule.

Au(111) were annealed.[178] A development of larger domain size was the apparent result of the heating and cooling. Thus, close-packing and high ordering of alkanethiolates on Au(111) may result from the relatively easy 2D "recrystallization" process, as well as from the above-mentioned migration of gold thiolate molecules.

Molecular mechanics (MM) energy minimization indicates that the two modes lead to monolayers exhibiting different types of packing arrangements (Figure 11), but comparable in their ground state energies. (The monolayer resulting from the sp^3 mode is more stable by 0.6 kcal mol^{-1}.[108]) Therefore, monolayers may consist of two different chemisorption modes ordered in different domains—simultaneously coexisting homogeneous clusters—each characterized by a different conformer in their unit cell. This may explain the observation of 2D liquid in butane- and hexanethiolate monolayers on gold,[177] where VDW interactions do not provide enough cohesive energy to allow for small domains to coexist as a 2D solid.

The chemisorption of S atoms,[188] SH,[189] and SCH_3 groups[190,191] on Ag(111) can be described as $(\sqrt{7}\times\sqrt{7})$-R10.9° (Figure 12), with an S···S distance of 4.41 Å, slightly smaller than the interchain repeat distance in crystalline paraffins of 4.65 Å.[192]

For octadecanethiolate ($CH_3(CH_2)_{17}S^-$) monolayers, GIXD shows a lattice constant of 4.6−4.7 Å, with alkyl chains that are hardly tilted, and an overlayer very similar to $(\sqrt{7}\times\sqrt{7})$R10.9°, but with 12° rotation, and an outmost Ag(111) layer slightly expanded.[193] Notice that the $(\sqrt{7}\times\sqrt{7})$R10.9° requires that the thiolates at the on-top site will be ∼0.5 Å higher than those residing at the hollow site. Dehirani *et al.* studied SAMs of decanethiolate ($CH_3(CH_2)_9S^-$) on Ag(111) using ultrahigh impedance STM.[194] They reported (a) that the average nearest-neighbor distance within a domain is 4.61 ± 0.15 Å; (b) that there are two domain types corresponding to two orientations of a 6-fold symmetric lattice separated by 20.7 ± 2.3°; and (c) that fluctuations of heights of nearest neighbors far from domain boundaries are less than 0.1 Å. In the $(\sqrt{7}\times\sqrt{7})$R10.9° structure, two possible domain orientations separated by 2 × 10.9° and 21.8° are predicted. Therefore, the structure of longer chain alkanethiolate SAMs cannot be the simple $(\sqrt{7}\times\sqrt{7})$R10.9° observed for the methanethiolate SAM. The structural change results from larger interchain VDW interactions, and from weakening the underlying Ag−Ag bonds as a result of the strong ionic character of the S−Ag bonds. Hence, a possible mechanism for interaction of longer alkanethiolate with Ag(111) is an initial formation of the $(\sqrt{7}\times\sqrt{7})$-R10.9° structure in early SAM formation stages. This, upon saturation of coverage, is followed by reconstruction of the silver lattice, and the increase in VDW interactions drive the packing of the alkyl chains to fall more into registry with each other, thus distorting the initial $(\sqrt{7}\times\sqrt{7})$ R 10.9° structure. The significant difference between the structure of methanethiolate and long alkanethiolates on Ag(111) is that the latter strongly influenced by the chain−chain VDW attraction. When a chain in an assembly of *all-trans* perpendicular chains moves vertically, there is a significant loss of VDW energy, unless the chain moves a C_n-C_{n+2} distance.[195] It was suggested before that VDW energy may be a driving force for reorganization of the substrate surface.[82] The case of alkanethiolates on Ag(111) is an example of this phenomenon, where molecules remain the same distance from the surface to maximize lateral interactions, thus bringing about reorganization of the silver outmost layer.

Some thiophenolate monolayers also have been investigated. Thiophenolate ($C_6H_5S^-$) forms ordered monolayers on Ag(111) with a $(\sqrt{7}\times\sqrt{3},88°)$R40.9°, and benzene rings closely packed in a face-to-face stacked columns.[196] Benzylthiolate,[197] *p*-pyridinethiolate,[197] and *o*-pyridinethiolate[197] also form ordered monolayers on Ag(111), but with less close-packed aromatic rings.

FTIR studies reveal that the alkyl chains in SAMs of thiolates on Au(111) usually are tilted ∼26−28° from the surface normal, and display ∼52−55° rotation about the molecular axis. This tilt is a result of the chains reestablishing VDW contact in an assembly with ∼5 Å S···S distance, larger than the distance of ∼4.6 Å, usually quoted for perpendicular alkyl chains in a close packed layer. On the other hand, thiolate monolayers on Ag(111) are more densely packed due to the shorter S···S distance. There were a number of different reports on chain tilt in SAMs on Ag(111), probably due to different amounts of oxide, formed on the clean metallic surface. Laibinis *et al.* suggested a value of 11−14°,[128] while Ulman suggested 7°,[127] and Nemetz *et al.*[198] and Fenter *et al.*[199] suggested that the chain are perpendicular to the surface. It is well accepted today that in carefully prepared SAMs of alkanethiolates on a clean Ag(111) surface the alkyl chains are practically perpendicular to the surface.

Functionalized alkanethiolate SAMs are important both for engineering of surface properties and for further chemical reactions. It is beyond the scope of this manuscript to review all reported functionalities. Suffice is to mention that simple—e.g., CH_3, CF_3, $CH{=}CH_2$, $C{\equiv}CH$, Cl, Br, CN, OH, OCH_3, NH_2, $N(CH_3)_2$, SO_3H, and $Si(OCH_3)_3$, COOH, $COOCH_3$, CONH2,[103−108,117,158,200,201]—as well as more complex functionalities—e.g., ferrocenyl,[166,202−209] biotinyl,[210−214]

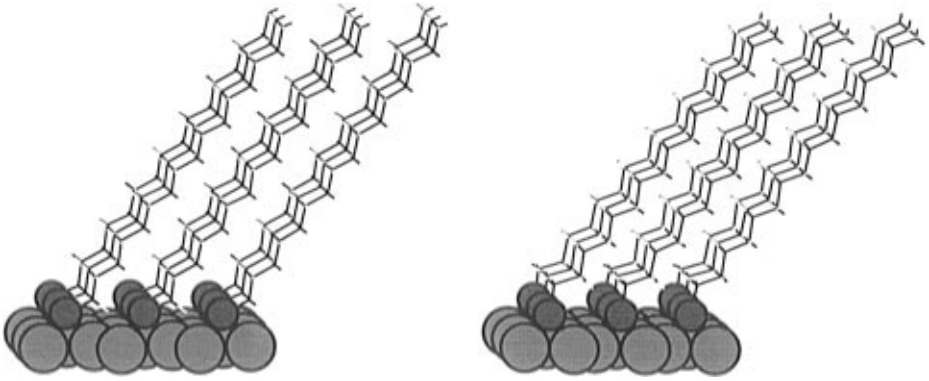

Figure 11. A view of the tilt in a nine-molecule section of a fully covered $SC_{16}H_{33}$ monolayer on Au(111) minimized with a modified MM2 force field including the sp^3 chemisorption parameters (left, calculated stabilization energy −23.29 kcal mol^{-1}) and with the sp chemisorption parameters (right, calculated stabilization energy −22.25 kcal mol^{-1}). The gold atoms are shown in light gray having their full van der Waals radii. The sulfur atoms are shown in dark gray and are not drawn to scale.

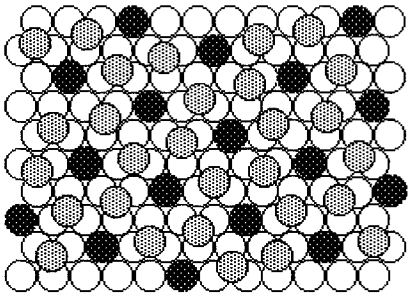

Figure 12. A diagram showing one of the two possible $\sqrt{7}\times\sqrt{7}$ structures of alkanethiolates on Ag(111). The open circles represent the silver atoms, while the dark- and light-shaded circles represent thiolates at the on-top and hollow sites, respectively.

2,2-bipyridyl,[215] tetrathiafulvalenecarboxylate,[216] tetraphenylporphyrin,[217,218] and ferrocenylazobenzene[219]—were attached to the chain termina of alkanethiolate monolayers. These monolayers are thus becoming the system of choice for studies of surface phenomena, electron transfer, molecular recognition, etc.

Surface OH and COOH are very useful groups for chemical transformations. Monolayers with terminal COOH functionality react with alkanoic acids[220] and decylamine[221] to form bilayer H-bonding-stabilized structures, which lack long-term stability due to the strong electrostatic repulsion in the newly formed charged interface. The carboxylate group can be transformed to the corresponding acid chlorides by using $SOCl_2$.[222] Further reactions with amines and alcohols yield bilayer structures with amide and ester linkages, respectively. Reacting the acid chloride with a carboxylic acid-terminated thiol provides the corresponding thioester. This reaction has been recently used by Kim *et al.* to form polymeric self-assembled monolayers and multilayers from the diacetylene $HS(CH_2)_{10}C{\equiv}CC{\equiv}C(CH_2)_{10}COOH$.[223]

SAMs of OH-terminated alkanethiols have been used in many surface modification reactions (Figure 13). They were reacted with OTS to yield a well-ordered bilayer,[224] with octadecyldimethylchlorosilane,[225,226] with $POCl_3$,[227−229] with trifluoroacetic anhydride,[230] with epichlorohydrin,[193] with alkylisothiocyanate,[231] with glutaric anhydride,[233] and with chlorosulfonic acid.[229]

4. Alkyl Monolayers on Silicon

Recently, Linford and Chidsey demonstrated for the first time that robust monolayers can be prepared where the alkyl chains are covalently bound to a silicon substrate mainly by C−Si bonds.[234,235] In the first experiments they used hydrogen-terminated silicon (H-Si(111) and H-Si(100)), and diacetyl peroxide.[234] The adsorption of alkyl chains was attributed to a series of free-radical reactions. In the first, a homolytic cleavage of the O−O bond occurs to form two acyloxy radicals:

$$[RC(O)O]_2 \rightarrow 2RC(O)O^{\bullet}$$

These radicals may decarboxylate to yield the corresponding alkyl radicals:

$$RC(O)O^{\bullet} \rightarrow R^{\bullet} + CO_2$$

Either the acyloxy or the alkyl radical abstracts a hydrogen from the H-terminated silicon surface to yield a dangling bond:

$$R^{\bullet} + H{-}Si(111) \rightarrow RH + {}^{\bullet}Si(111)$$

Finally, this surface radical combines either with the alkyl or with the acyloxy radical to give the Si−R or Si−O(O)CR species, respectively. It was found that these monolayers, although exhibiting thickness, wettability, and methylene stretching frequencies indicative of highly packed chains, lost ∼30% of the chains when exposed to boiling water. The apparent conclusion was that hydrolyzable acyloxy groups are removed, leaving the robust alkyl chains bound to the surface by the C−Si bonds.

In an attempt to reduce the fraction of surface acyloxy groups, a mixture of alkene and diacetyl peroxide was used.[235] Reaction of alkynes also yielded robust, closely packed monolayers and chlorine-terminated olefins gave monolayers with wettability indicative of Cl-terminated alkyl chains. The resulting monolayers are ∼90% olefin-based as shown by deuterium-labeling experiments. The introduction of olefin molecules can be explained by a radical reaction in which the surface radical (dangling bond) reacts with the double bond to yield a secondary carbon radical:

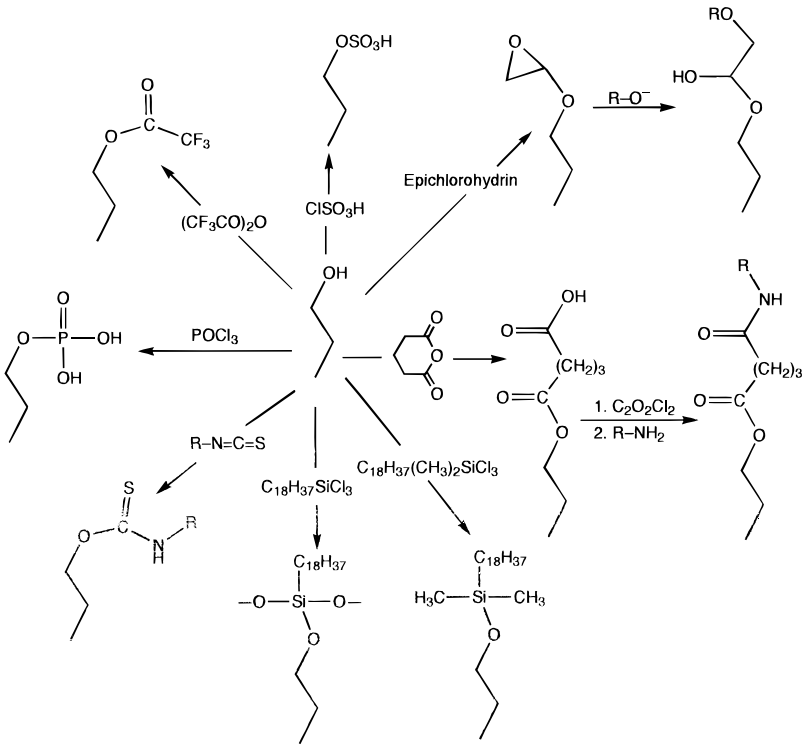

Figure 13. Surface reactions of ω-hydroxyalkanethiolate monolayers on Au(111).

$$R'CH{=}CH_2 + {}^{\bullet}Si(111) \rightarrow R'CH({}^{\bullet}){-}CH_2{-}Si(111)$$

This radical can either abstract another hydrogen from the allylic position of an olefin molecule:

$$R'CH(\bullet){-}CH_2{-}Si(111) + R'CH_2CH{=}CH_2 \rightarrow R'(CH_2)_2\ Si(111) + R'CH({}^{\bullet})CH{=}CH_2$$

or with a surface Si−H group:

$$R'CH({}^{\bullet}){-}CH_2{-}Si(111) + H{-}Si(111) \rightarrow R'(CH_2)_2\ Si(111) + {}^{\bullet}Si(111)$$

The monolayer density, as measured by X-ray reflectivity, is only ~90% of the value of a crystalline paraffin such as n-$C_{33}H_{68}$, suggesting a significant number of defects. Ellipsometry and infrared spectroscopy suggest that the chains are tilted ~45° from the surface normal, and that a twist angle of ~53° exists between the plane that bisects the methylene groups and the plane of the tilt. This tilt angle is not surprising since the interchain distance is 6.65 Å.[195]

While monolayers of alkyl chains on silicon are in their very beginning, they clearly are a significant addition to the family of SAMs. An ability to directly connect organic materials to silicon allows a direct coupling between organic materials and semiconductors. The fine control of superlattice structures provided by the self-assembly technique offers a route for building organic thin films with, for example, electrooptic properties on silicon.

5. Multilayers of Diphosphates

One logical way to finding surface reactions that may lead to the formation of SAMs is to look for reactions that result in an insoluble salt. This is the case of phosphate monolayers, based on their highly insoluble salts with tetravalent transition metal ions. In these salts, the phosphates form layer structures, with one OH group sticking to either side. Thus, the idea was that replacing the OH with an alkyl chain—forming the alkyl phosphonic acid—should result in a bilayer structure with alkyl chains extending from both sides of the metal phosphate sheet.[236] Interestingly, when zirconium is used (Zr^{4+}) the distance between next-neighbor alkyl chains is ~5.3 Å, which forces either chain disorder or chain tilt so that VDW attractive interactions can be reestablished.

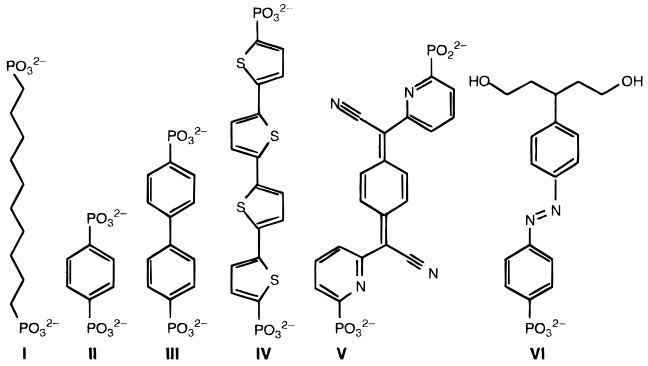

Figure 14. Different diphosphonic acids used in self-assembled multilayer preparation.

Mallouk pioneered this area when discovering that self-assembled multilayers can be prepared simply by alternating adsorption of Zr^{4+} ions and α,ω-alkylidene diphosphate (I) on a phosphorylated surface.[237,238] Other diphosphates have since been investigated (Figure 14), for example, 1,4-benzene (II),[226,227] 4,4′-biphenyl (III),[239] and quaterthienyl (IV).[239,240] More complex molecules also were investigated, for example, 7,8-dicyano-7,8-bis-(*o*-pyridyl)-*p*-benzoquinonedimethide (V), bipyridine salts, [241] and porphyrins.[241]

So far we have discussed centrosymmetric multilayers; however, for second-order NLO applications, the films needs to be noncentrosymmetric and therefore diphosphates cannot be used. Katz has used [[4-[bis(2-hydroxyethyl)amino]phenyl]azo]benzenephosphonate to form SAMs on zirconium-treated phosphorylated surfaces. Further reaction with $POCl_3$ and hydrolysis created a new phosphorylated surface that could be treated with zirconium salt, etc.[242−244] The major advantage of the phosphate systems is in their high thermal stability, their simple preparation, and the variety of substrates that can be used. The latter is especially important if transparent substrates are required, since it is not possible in the case of thiolate monolayers, and alkyltrichlorosilanes have a serious stability disadvantage.

III. Competing Interactions in the Formation of Self-Assembled Monolayers

Organization of complex, semiflexible organic molecules within quasi 2D assemblies is the result of a delicate interplay between substrate−adsorbate interactions, nonbonded interactions between adsorbates—electrostatic and VDW forces—and intramolecular interactions such as bond stretches, angle bends, and torsions. Surface reorganization contributes to the final equilibrium structure of the assembly. In the following parts of this review, we discuss the competing interactions in the formation of SAMs and try to provide a general understanding of the issues one should consider when designing a new SAM.

1. Why are Alkanethiolates on Au(111) and Ag(111) Different?

The difference between alkanethiolate SAMs on Au(111) and Ag(111) surfaces is striking, especially when regarding that the nearest-neighbor distance in the two lattices are so similar (2.88 and 2.89 Å, respectively.) If one considers that iodine forms a $(\sqrt{3}\times\sqrt{3})$R30° structure on Ag(111), with the iodine atoms occupying the hollow sites, the structural differences between of alkanethiolate SAMs on Au(111) and on Ag(111) must result from an interplay of chemisorption and chain−chain interactions. Silver is more reactive than gold, it forms an oxide spontaneously, its oxidation potential is 1.7 eV lower, and its work function 0.6 eV lower. Gold and silver also differ—due to relativistic effects[108]—in the peak-to-valley roughness at their [111] lattices, 6.0 kcal mol^{-1} for Au(111) (Figure 15), and only 3.3 kcal mol^{-1} for Ag(111).[108] Therefore, even if an Au(111) or an Ag(111) surface is atomically flat, it is energetically heterogeneous, which results in site selection of adsorption.

As mentioned above, thiolates on Au(111) occupy every sixth hollow site, resulting in a $\sqrt{3}\times\sqrt{3}$R30° overlayer,[172−174] that is commensurate with the underlying Au(111) lattice (Figure 9). However, because in Ag(111) the energy difference is smaller than in Au(111), adsorption at an on-top site in the former may compete with that at the hollow site. Figure 15 is a sketch of optimum interaction energy of a single thiolate at different *x*,*y* coordinates on a (111) surface of either gold or silver. The interaction energy is large and negative for all *x*,*y* points (∼−44 kcal mol^{-1} [103]). Superimposed on that is a regular roughness, indicating site discrimination. The depressions correspond to the most favored binding sites (hollow sites, Figure 9), and the peaks are the least favored sites (on-top positions, Figure 12).

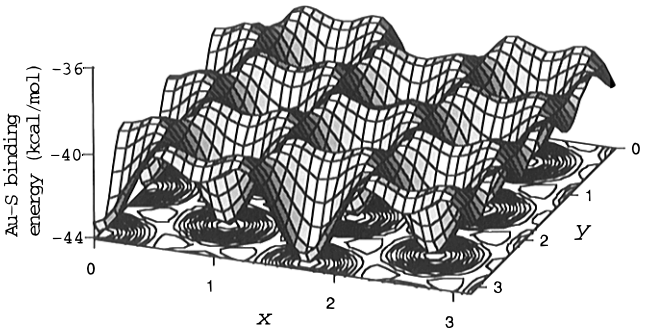

Figure 15. A schematic view of the binding energy surface for thiolates on Au(111). Energy maxima represent on-top sites, and energy minima represent hollow sites.[108]

As suggested by Outka *et al.*,[245] and discussed by Ulman *et al.*,[195] only certain combinations of chain−chain separation (i.e., lattice spacing) and tilt angles permit truly effective packing of alkyl chains. The most effective packing is a trigonal lattice with spacing near ∼4.4 Å with a molecular axis normal to the surface.[195] This distance (4.41 Å) was found for methanethiolate on Ag(111); however, for longer alkyl chains the distance of ∼4.6 Å has been reported.[193−194] The second most effective has a spacing near 5.0 Å and the molecular axis tilted ∼30°, such that the distance between the chains is, again, ∼4.4 Å and the fit of bulges into depressions is again perfect. It can be thought of as a ratchet that has slipped by precisely one notch (Figure 11). In alkanethiolate monolayers on GaAs, the ratchet has slipped by two notches, resulting in a tilt angle of 57°.[140] A second consideration is that crowding more molecules per unit surface area will result in both more chemisorption energy and VDW attraction for the entire system simply because there are more chains involved. This is a lot of energy, since the possibility of adsorption at on-top sites means that in SAMs of thiolates on Ag(111) there are 26% more chains per unit area than on Au(111) on-top sites.[108] Recent surface coverage measurements using radiolabeled octadecanethiol confirm this loading difference.[164] Why then does chemisorption of thiolates on Au(111) show such a clear site selection? This is because the above effects are partially offset by the charge−charge repulsions both among S and Au atoms. If a $(\sqrt{7}\times\sqrt{7})$R10.9° overlayer of methanethiolate on Au(111) existed, every seventh gold atom (occupied on-top sites) would have a positive charge of ∼+0.7e, while the others would have about +0.4e/3, as all gold atoms in the $\sqrt{3}\times\sqrt{3}$R 30° overlayer scheme. Hence, chemisorption potentials with significant lateral discrimination could counter the favorable effects of interchain interaction energy. It is the combination of lateral discrimination and electrostatic effects that distinguishes the chemisorption of thiolates on Au(111) from that on Ag(111). In the following discussions we address issues of intermolecular interaction. We start by analyzing the spontaneous formation of a 2D assembly.

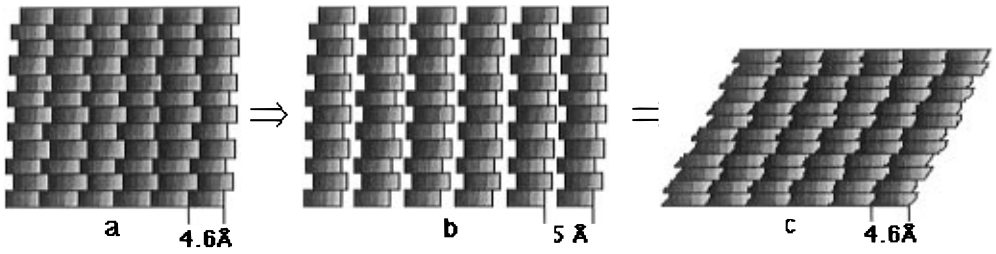

Figure 16. A schematic representation—not drawn to scale—of brick strata perturbed from close packing by the introduction of a single stratum with spacing larger than the block size. Intrastrata interactions are weaker than interstrata interactions, while are, essentially, chemical bonds. The free volume can be eliminated by tilting the brick columns in b thus reestablishing contact. Notice that the shape of the bricks changed, and while their volume is the same, their thickness is now the projection of the interstrata bond on the surface normal. The broken line represents monolayer thickness.

2. The Interlocking of Molecular Parts

In trying to understand the packing and ordering of complex molecules in SAMs, the questions are (a) what are the parameters that control *spontaneous* layer formation? and (b) how adsorbate−adsorbate interactions are affected by the chemisorption scheme at the surface? and *vice versa*. In considering the formation of a 2D assembly from complex molecules, intermolecular interactions are first considered independently. Similar to 3D molecular crystals that have been viewed and analyzed as an assembly of commensurate 2D molecular layers, 2D assemblies are considered as a structure of commensurate intraassembly planes.[246,247] If the molecule consists of aromatic rings and alkyl chains, the contribution of these parts to the equilibrium molecular packing and ordering in the SAM must be understood. Simple planar π-systems tend to spontaneously aggregate in layers, usually with herringbone structures. Similarly, paraffins spontaneously assemble in pseudohexagonally close-packed layer structures. In both cases there usually is more than one possible stable packing arrangement, and in some cases these arrangements have about the same stabilization energy.[246] Forming a chemical bond between the π-system and the alkyl chain results in a more complex molecule, and it is not clear *a priori* if this will spontaneously self-assemble in a layered structure. Some molecules do form stable 2D layers, while others undergo bulk crystallization.

The factors that determine formation of layered structures of complex molecules are (a) that cross sectional area mismatch of different molecular parts is minimal; (b) that intraassembly planes that are defined by different molecular parts are commensurate, i.e., an epitaxial matching of the sublattices of different intraassembly layers exists; and (c) that bonds between different molecular parts do not perturb a and b. A complex molecule will spontaneously form a layer structure if this results in none, or very little, perturbation in the layer structure of its components. This principle is best manifested in smectic liquid crystals of biphenyl derivatives. Calculations show that cross sectional areas match, that 2D intraassembly planes are commensurate,[246] and that the chemical bonds between the π-system and alkyl chains do not cause any disruption of the assembly.

In reality, many molecules consist of parts that are making lattices that are incommensurate. There, the stability of the layered assembly can be augmented by chemisorption—self-assembly—on a solid surface. Thus, although the unconstrained layered structure is not in a global minimum of free energy, there are mechanisms that may yield a layered assembly that is in a global minimum. These mechanisms involve intra and intermolecular interactions, the results of which is closer molecular packing and higher order. To understand how a spontaneous layer formation comes about, one needs to consider intermolecular interaction in greater detail, and consider a 2-D assembly of alkyl chains as formed by strata of close-packed methylene (CH_2) units.

An alkyl chain may be viewed as a segment of a 1D crystal, simply because of the constant distance (2.52 Å) found between second-nearest-neighbor carbon atoms. Likewise, 2D assemblies of packed alkyl chains, where coplanarity is enforced, might be viewed as stacks of microlayers or strata, where each stratum is comprised of closely packed atomic groups, i.e., CH_2 units. Figure 16 shows a schematic representation of brick strata. Each brick represents one CH_2 unit, and a column of brick represents an alkyl chain. Consider an ideal monolayer system composed of straight alkyl chains, attached to an atomically flat substrate, with a repeat distance of ~4.6 Å (Figure 16a).

In this assembly, intrastratum packing energy is minimized without putting any strain on individual molecules. The system can be perturbed by introducing a single stratum with spacing larger than ~4.6 Å, with symmetry different than triagonal, or with blocks that have a smaller/larger unit size. For example, one could create a perturbed system by moving the attachment points from ~4.6 Å—as for alkanethiolates on Ag(111)—to ~5 Å—as for alkanethiolates on Au(111) (Figure 16b). As a result, close packing can no longer be present for undistorted vertical chains. In the perturbed system, packing requirements of the perturbing stratum (bottom in this case) and those of other strata conflict. The system accommodates the conflicting demands by tilting the chains over in such a way as to reestablish optimum VDW contacts within and between strata (Figure 16c).[195]

3. Alkanethiolates on Au(100): A Different Symmetry

Alkanethiolate monolayers on Au(100) were studied using electron diffraction[172] and helium diffraction.[248] While the former established that the thiolates adsorb in a simple square symmetry with S···S spacing of 4.54 Å, the latter did not find the terminal methyl groups organized either in square or hexago-

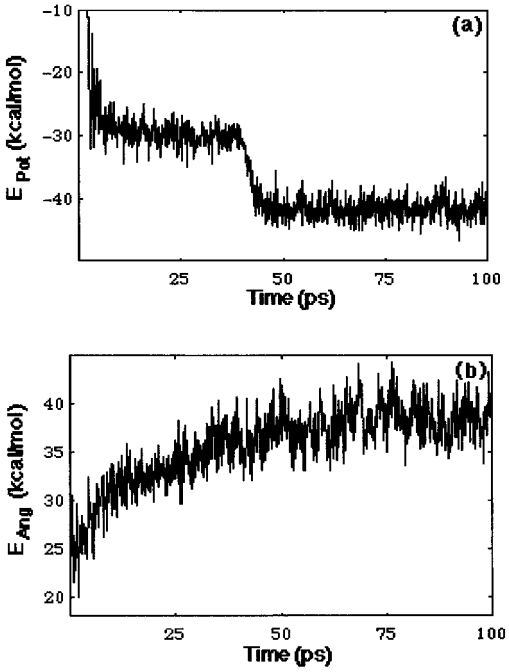

Figure 17. Time evolution of various contributions to total energy in the MD trajectory of the docosanethiolate monolayer on Au(001). The total VDW energy and total bond stretch energy are represented by a and b, respectively.

nal symmetry, and X-ray diffraction studies established a rather complex, distorted hexagonal chain packing. Clearly, the introduction of a stratum of S atoms with a symmetry different from that preferred by alkanes resulted in molecular reorganizations that are reflected in the packing and ordering of the surface methyl groups. Early on, before the full structure analysis of alkanethiolates on Au(100) was complete, Ulman and co-workers carried out molecular dynamics (MD) simulations with two assumptions: the first, a square adsorption symmetry with a 5.54 Å S···S distance, and the second, that all thiolate sulfurs form a plane.[14] While the latter has been shown to be incorrect, it is worthwhile to discuss briefly the MD results since they provide a possible mechanism for the formation of the observed structure.

MD simulations of a docosanethiolate ($CH_3(CH_2)_{21}$-SH) monolayer on Au(100) suggests that the chains are tightly packed and exhibit very little thermal disorder.[14] Time evolution of selected energy components shows that the onset of equilibration coincides with an abrupt decrease in the total VDW energies (Figure 17a).

This is the result of CH_2 units locking into an optimal close-packed arrangement within and between the strata. On the other hand, a gradual increase in total angle bend energy and torsional energy—resulting from increased chain distortions—is evident (Figure 17b). The nature of these distortions can be seen in Figure 18, where Figure 18a exhibits both a concerted lean (~30°), and a mild bending distortion of the chains, while Figure 18b—a view parallel to the other face of the simulation cell—shows that alternating rows of chains acquire a staggered ~5° tilt. (The tilt is defined as an angle from the normal within the plane that bisects the methylene groups, and the lean as the angle from the normal in a plane perpendicular to it.) Notice, that while in alkanethiolate monolayers on Au(111) there is a tilt of ~30° and a lean of ~22°,[249] in monolayers on Au(100) the tilt is ~5° and the lean ~22°. The tilt and lean result from the relationship between molecular spacing and the dimensions of the methylene group, the latter being oval in shape with a ratio of ~1.13 between the two axes.

It was argued before[195,245] that tilt of alkyl chains should obey the formula $\phi = nR/D$, where ϕ is the tilt angle, $R = 2.52$ Å, D is the minimum VDW separation between the chains (4.45 Å from crystallographic data[192]), and $n = 0, 1, 2$. While carrying out only preliminary calculations, we suggest that a corresponding formula should exist for the lean. The choice of molecular orientation within the assembly is determined by the best combination of tilt and lean. In the lean, the VDW interactions are mainly H···H, while in the tilt there is a significant contribution from C···C interactions. Therefore, it can be assumed that the larger contribution to the VDW energy comes from the tilt and that it should be the dominating factor in determining molecular orientation. In the present case, the S···S distance is 4.54 Å, leaving very little free volume in the tilt direction. In the other direction, where the dimension of the methylene group is smaller, the difference between the distance and the group dimension is the same as the distance between the rows of chains on Au(111). Both there, and in this case, using the same MM calculations, a lean of ~22° was found, provided that the chains are undistorted and adopting an *all-trans* conformation. Interestingly, a stratum-by-stratum examination reveals a nearly hexagonal close packing in the middle strata—confirming that the minimum energy is a distorted hcp structure—and a disordered hexagonal arrangement at terminal methyl stratum. Figure 19 shows that a stratum of methylenes packed in a square lattice can be deformed toward a trigonal hcp arrangement by the sliding of alternate rows of methylenes. The tilting of alternate rows seen in Figure 18b affects this kind of deformation in the individual strata. The chemisorption and intramolecular bonding constraints restrict the magnitude of sliding.

A schematic real space mesh of the c(2×8) top surface structure proposed from helium diffraction data is presented in Figure 20.[248] Notice the two kinds of methyl groups with different heights. These are the result of alkanethiolate adsorbed at the on-top sites of the Au(100) lattice, as can be seen in Figure 21. That in SAMs of alkanethiolates on Au(100) there should be two kinds of adsorbed thiolates has been suggested by Sellers and coworkers.[108] The molecular tilt angles that best fit the Bragg rod profiles are 33.5 ± 1.0° in a direction and 6.8 ± 1.0° away from the elongated next-nearest-neighbor (NNN) direction. This is close to that of octadecanethiolates on Au(111).

The similarity between the chain packing in alkanethiolate SAMs on Au(111) and Au(100) is surprising, given the symmetry difference in the adsorption schemes. While the observed tilt angles differ from the MD simulation predictions, the observation of a distorted hexagonal chain packing is in agreement with the simulations. This is an indication that the equilibrium structure of a SAM is the result of a

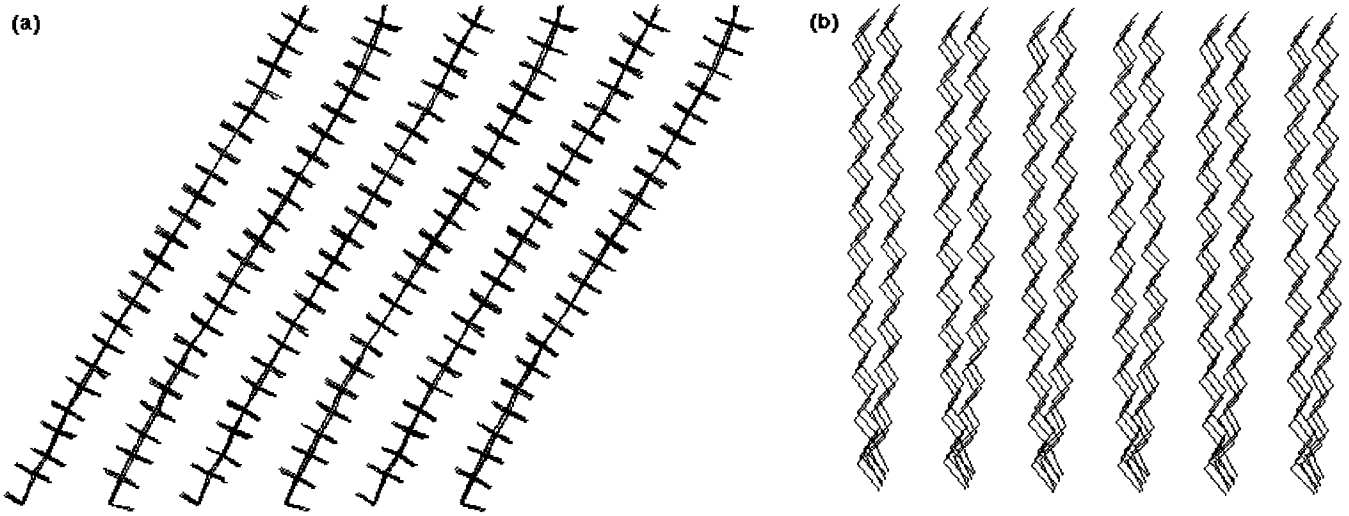

Figure 18. Two side views of a typical low-energy snapshot from the equilibrated portion of the MD trajectory (t = 83.7 ps).

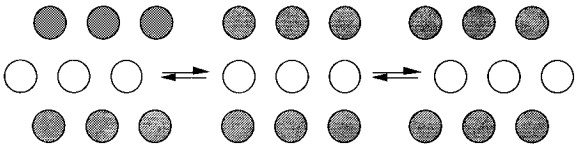

Figure 19. Deformation of a square lattice of methylene groups toward a trigonal hcp lattice by sliding alternate rows of methylene groups.

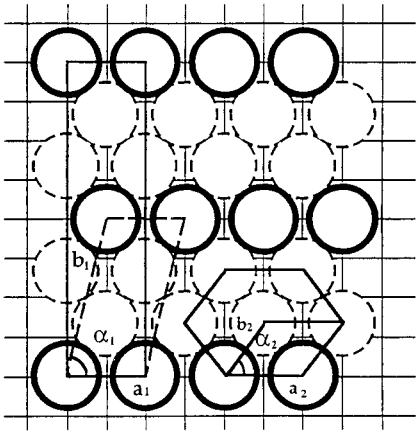

Figure 20. The comparison of the real space mesh suggested by helium atom diffraction and X-ray diffraction. The square meshes represent the ideal Au(100) truncation surface lattice. Each alkanethiolate is represented by an open circle. Both of the c(2×8) unit cell (thick lines, and the oblique primitive unit cell (dashed lines) by atom diffraction are plotted out. The distorted hexagonal cell derived by X-ray diffraction is a subunit of the c(2×8) cell. The dashed circles are different from the others at topmost surface. (from ref 248. Copyright 1993 American Institute of Physics.)

delicate balance between competing forces. In the case of alkanethiolates on Ag(111) interchain interactions drive the reorganization of the outmost silver atoms layer. Similarly, the packing and ordering of alkanethiolates on Au(100) are driven by minimizing intra- and interchain energy. That hexagonal close packing provides the best arrangement of alkyl chains in space is a major driving force for the reorganization predicted by the MD simulations and observed in the X-ray diffraction studies. Furthermore, the increase in intramolecular energy imposed by the reorganization, as predicted by the MD simulations, may be the driving force for the apparent mixture of molecular heights. Since the adsorption at an on-top site is the least stable,[108] the elimination of potential intramolecular energy increase should offset the decrease in chemisorption energy. The existence or absence of molecular distortion as depicted in Figure 18 cannot be detected using X-ray diffraction, and FTIR may not be sensitive enough to detect small changes in individual bond angles even if they result in a significant overall change. The chain twist about its axis provides the final molecular adjustment and the equilibrium structure is established.

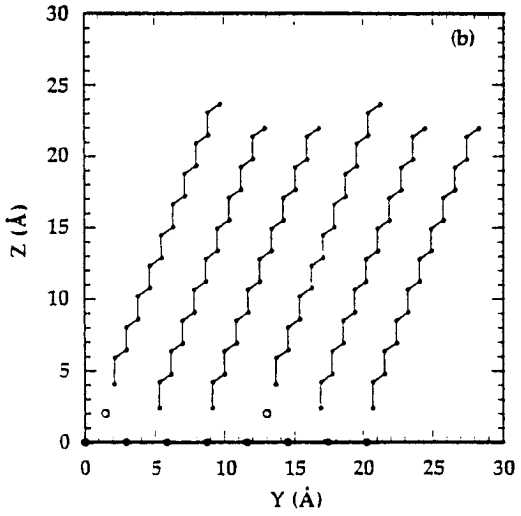

Figure 21. The YZ projection of alkanethiolates adsorbed at an Au(100) surface. Interfacial Au atoms are represented by the open circles. The substrate Au atoms are represented by the filled circles. The alkyl chains are assumed to be *all-trans* zigzag backbones. Only sulfur and carbon atoms are shown. (from ref 248. Copyright 1993 American Institute of Physics.)

5. Specific Intermolecular Interactions in SAMS

Introduction of specific interchain interactions may lead to control of the 2D structure of the SAM. This may drive 2D crystallization and result in enhanced packing and ordering. Dipole−dipole or H-bonding interactions may be designed by introducing sulfone or amide groups into the alkyl chain, respectively.

Ulman and co-workers studied both experimentally[147] and with the use of MD simulations[14] the

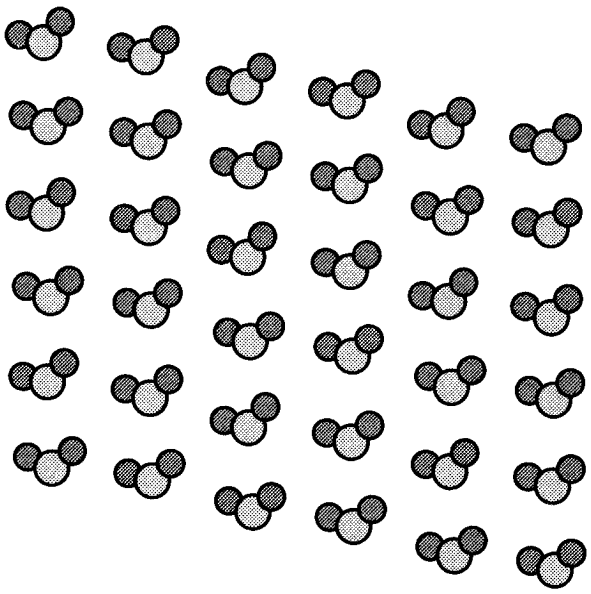

Figure 22. A top view of the packing of SO_2 groups within a $CH_3(CH_2)_7SO_2C_6H_4O(CH_2)_8SH$ SAM on gold. Note the two-dimensional ordering of the dipoles.

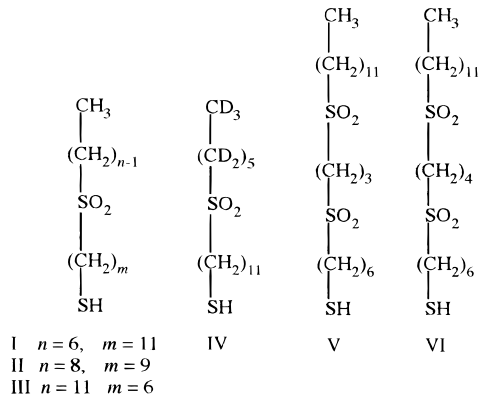

Figure 23. Sulfone-containing alkanethiols.

SAMs of $CH_3(CH_2)_7SO_2C_6H_4O(CH_2)_8SH$ on gold. It was noticed that the sulfone ($-SO_2-$) groups form a layer that practically does not change during the MD run (Figure 22). The formation of this layer is driven by dipole−dipole interactions among the sulfone groups.

Further studies revealed that the introduction of sulfone groups with large in-plane dipoles into alkanethiols (Figure 23) has very little effect on molecular conformation within the resulting SAM and that the molecules are in the *all-trans* conformation. However, these in-plane dipoles have a profound effect on molecular tilt, i.e., the molecules tilt in one direction only. Such a molecular tilt is in contrast to that which exists in assemblies of simple alkanethiols on Au(111).[250] Evidently, this molecular tilt is the result of the strong $SO_2\cdots SO_2$ electrostatic interactions that promote the formation of a plane of dipoles within the assembly. Hence, the introduction of a plane of dipoles within the assembly affects the packing and ordering of the monolayers and provides a mean by which dipolar interactions within molecular assemblies may be studied. A general trend was observed from the wetting behavior of these films, which the contact angles decrease as the length of the chain above the sulfone group is reduced. This can be interpreted in two ways: (a) the disorder near the surface could be increasing, and/or (b) the dipolar interactions due to the polar sulfone become more prominent. IR data indicates that the disorder resulting from the incorporation of the sulfone groups is the primary cause. In considering the differences in the wetting behavior between these and alkanethiolate SAMs, a third factor must also be taken into consideration. Since the polarizability of a hydrocarbon chain is anisotropic, then if such molecules display a preferred direction of tilt, they will present a surface with a different degree of polarizability than that obtained from a surface with no preferred direction of tilt.

It seems quite remarkable that the $-SO_2-$ groups perturb the monolayer so little relative to the monolayers without them, considering their size. Obviously, the sulfone groups perturb in-layer close packing of the alkyl chains due to the introduction of free volume, but this perturbation is compensated by the ordering induced through the dipole−dipole interactions.

Whitesides *et al.* have studied SAMs on gold from alkanethiolate with the structure $RNHCOCH_2SH$.[251] They found that the intermolecular H-bonding in SAMs prepared from $CF_3CH_2NHCOCH_2SH$ increases their stability against desorption or exchange with hexadecanethiol in ethanol relative to SAMs from $CF_3(CH_2)_3SH$. The remarkable stabilization effect of H-bonding is evident from the apparent lack of desoption from $CF_3CH_2NHCOCH_2SH$ SAMs after 48 h at $\sim 10^{-9}$ Torr. In comparison, the desorption from SAMs from $CF_3(CH_2)_3SH$ had a half-lifetime of $\sim$2 h at $\sim 10^{-9}$ Torr, with first-order kinetics. The exchange rate with hexadecanethiol was 10^2-10^3 slower for the amide-containing SAMs. FTIR studies established that the organization of alkyl chains within these SAMs is unlike that found in alkanethiolate SAMs.

The $-SO_2-$ and $-NHCO-$ groups, while different in their mode of action, represent the significance that introduction of structural motifs may have on the structure and stability of SAMs. Understanding how different groups may influence packing and ordering is important for future design of supramolecular structure with engineered physical properties. Certainly, much more needs to be done in this area.

6. Surface Engineering Using SAMs

Independent control of surface structure and chemical properties and the resulting structure−property relationships are both scientifically interesting and technologically important. For many applications, controlling the properties of interfaces is very important. However, in real-life circumstances, interfaces that contain at least one polymer surface are typically irregular. Surface properties of polymers depend critically upon the chemical and physical details of molecular structure at the surface of the polymer. To control surface properties by manipulating surface structure, it is necessary to have an extensive database of detailed correlations between properties and structure for the polymer surface of interest. However, other than generalizations about simple behavior (e.g., wetting and chemical reactivity), very little definitive work has been reported on such structure−property correlations for polymer surfaces.

Since surface properties are generally considered to be controlled by the outmost 5−10 Å at a polymer film,[252] a logical solution is to use self-assembled monolayers (SAMs) as model polymer surfaces. To fully understand the breadth of surface interactions, one needs a portfolio of chemical functionalities so that different surface forces can be tailored at the molecular level. SAMs are especially suited for the studies of interfacial phenomena due to the fine control of surface functional group concentration. These surfaces can be produced to have surface energies which span the range from "Teflon-like" surfaces (surface CF_3 groups) to very high energy surfaces (surface OH or COOH groups), i.e., surface tensions of 10−70 dyne cm^{-1}.

For example, SAMs with variable lengths of alkyl chain can be used to screen the interactions of a polymer with an underlying substrate. Charged surface functionalities can be used to study the Debye screening length in processes such as protein adsorption. Polar surfaces, with groups such as cyano (C≡N), can be used to investigate the contribution of dipole−dipole interactions in surface adhesion. Surface OH groups can vary wetting behavior and provide insight into the importance of H-bonding in surface phenomena.

When choosing a SAM system for surface engineering, there are several options. Silane monolayers on hydroxylated surfaces[1] are an option, when transparent or nonconductive systems are needed. However, trichlorosilane compounds are moisture sensitive and polymerize in solution, with the resulting polymers contaminating the monolayer surface that occasionally has to be cleaned mechanically. Carboxylic acids adsorb on metal oxide (e.g., Al_2O_3, AgO) surfaces through acid−base interactions.[1] These are not specific; therefore, it would be impossible to selectively adsorb a carboxylic acid in the presence of, for example, a terminal phosphonic acid group. Therefore, in many studies SAMs of thiolates on Au(111) are the system of choice.

The structure of SAMs is affected by the size and chemical properties of surface functionalities. In fact, the introduction of any surface functionality reduces monolayer order. The driving force for disorder may result from sterically demanding terminal groups, e.g., $-OSi(CH_3)_2(C(CH_3)_3)$,[143] and $-C_5H_5N{:}Ru(NH_3)_5-$,[253,254] or from very polar surface groups, e.g., OH, COOH, etc. In both cases, the introduced disorder may be significant and not confined only to the surface.

The sensitivity of wetting to surface chemistry is evident from an OH concentration-driven wetting transition of hexadecane (Figure 24),[6] observed in the studied of mixed SAMs containing varying proportions of hydrophobic (CH_3) and hydrophilic (OH) components. A mechanism based on the influence of surface-adsorbed water layers was supported by calculations based on a mean-field Cahn-type wetting analysis. These calculations also predicted the correct trend in the transition-onset position as a function of relative humidity.[255] As relative humidity decreases, the transition-onset shifts to higher surface OH concentration. This prediction was confirmed experimentally (Figure 24). In an experiment demonstrating the sensitivity of the wetting process

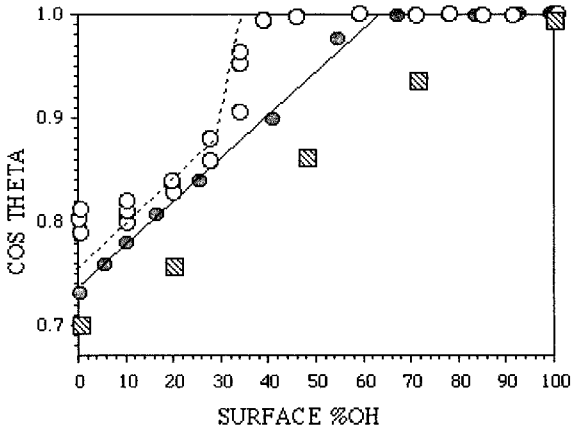

Figure 24. The cos θ of hexadecane for $HO(CH_2)_{11}SH$ and $CH_3(CH_2)_{11}SH$ in 30% RH (open circles) and in ≤2% RH (gray circles), and for $HO(CH_2)_{11}SH$, and $CH_3(CH_2)_{13}SH$ (squares) mixed alkanethiolate SAMs on gold, as a function of surface OH concentration. Theoretical calculations are shown as lines.

to surface roughness at the molecular level, two CH_2 groups (together, 2.5 Å long) were added to the hydrophobic component. The wetting transition disappeared (Figure 24). This remarkable observation demonstrates the potential of surface engineering using SAMs, where changes at the molecular level made possible by utilizing mixed SAMs may result in control of macroscopic surface properties. However, the success of surface engineering at the molecular level requires surface stability, i.e., that surface functional groups do not initiate and promote surface reorganization. Moreover, since it can be expected that structural changes at the surface will penetrate into the monolayer bulk, surface stability may have a significant effect on the equilibrium structure of the monolayer. Surface reorganization is a complex phenomenon, and it is not clear *a priori* to what depth conformational changes that start at the surface will penetrate. Nevertheless, one could expect this depth to be a function of monolayer viscosity, i.e., molecular chain length.

Instability in the wettability behavior of OH surfaces was noticed when OH-terminated silane monolayers where exposed to hydrophobic solvents, such as CCl_4.[61] Similarly, monolayers of 11-hydroxyundecanethiol ($HO(CH_2)_{11}SH$, HUT) on Au(111) surfaces have been found to undergo surface reorganization by exposure to ambient atmosphere for few hours.[230] After that, the water contact angle reached a value of ∼60°, and only ∼25% of the OH groups could be esterified by trifluoroacetic anhydride. Molecular dynamics simulations performed by Klein *et al.* verified that the driving force for the surface reorganization is the formation of surface-correlated H-bonds.[256,257] Surface instability was also observed for mixed monolayers, and it was found that the decrease of surface free energy with time increases with the increasing number of surface OH groups, i.e., with the increase of surface free energy. These observations support a mechanism in which surface free energy decreases due to the decrease of surface OH groups, resulting from conformational changes at chain termina. As surface free energy increases, the driving force for reorganization, which results in exposure of CH_2 groups and surface energy decrease, increases. This driving force can be offset by strong

intermolecular interactions. Stability studies of monolayers made of a longer chain derivative, $HO(CH_2)_{21}SH$, as a function of temperature showed that surface reorganization is indeed a function of monolayer melting point.

Every monolayer surface, even that made of CH_3 groups, is disordered at room temperature because of gauche defects at the chain termina. However, it should be recognized that while the concentration of surface gauche defects is a function of free volume, the latter is a function of the adsorption scheme and of molecular cross sectional area. Furthermore, surface reorganization may be augmented by the formation of H bonds, as in the case of surface OH groups, or be restricted by the size and shape of the functional group (OH vs COOH or SO_3H). Temperature, relative humidity, and adsorption at the monolayer surface are other factors that affect surface stability. The equilibrium structure of a surface is the result of balancing all these factors and is very hard to predict. However, the stability of a monolayer against reorganization may be increased by intermolecular interactions as described above; however, studies confirming this hypothesis have not been carried out yet.

IV. Conclusions

Organization of complex, semiflexible organic molecules within quasi 2D assemblies is the result of a delicate interplay between substrate−adsorbate interactions, nonbonded interactions between adsorbates−electrostatic and VDW forces−and intramolecular interactions such as bond stretches, angle bends, and torsions. Surface reorganization contributes to the final equilibrium structure of the assembly.

Research in SAMs had originally been driven by their potential application as building blocks for superlattices with engineered physical properties. However, due to the relatively long adsorption process, SAMs cannot compete with existing technologies even when the figure of merit for device performance is higher. Thus, the more immediate contribution to science and technology will come from their utilization in surface engineering. One example of a potential technology is semiconductor surface patterning. Calvert and co-workers have used silane derivatives,[258] while Whitesides and co-workers have demonstrated the utility of alkanethiol monolayers.[165,259] Another important example is transducer technology, where optical, piezoelectric, and other forms of chemical sensors have been demonstrated using SAMs.[260] In this context, Raman spectroscopy is an attractive means of detection, when coupled with the unique interfacial SAM properties.[261] Surfaces of piezoelectric devices have been modified with SAMs.[262] There, engineering of donor−acceptor, hydrophilic−hydrophobic, and complexation properties via tailoring chain termina functionalities leads to detection of gaseous analytes.[263,264]

Electroanalytical chemistry was one of the areas where advantage of the unique properties of SAMs is clear, and where excellent advanced analytical strategies can be utilized, especially when coupled with more complex SAM architectures. There are a number of examples where redox reactions are used to detect biomaterials,[265,266] and where guest−host chemistry has been used to exploit specific interactions.[264,267] Ion-selective electrodes is another application where SAMs may provide new technologies. Selectivity to divalent cations such as Cu^{2+} but not to trivalent ions such as Fe^{3+} has been demonstrated.[268]

Future development of SAM-based analytical technology requires expansion of the size and shape selectivity of template structures, as well as introduction of advanced chemical and optical gating mechanisms. Another important contribution of SAMs is in miniaturization of analytical instrumentation. This may have considerable importance in the biomedical analytical area, where miniature analytical probes will be introduced into the body and target specific organs or even cell clusters. Recent advances made in Whitesides' group in high-resolution spatial patterning of SAMs open the way for such technologies.[165,259]

Another area where contributions can be made using SAMs is in the molecular level understanding of surface phenomena. For many applications, controlling the properties of interfaces is of primary importance. The lubrication of moving parts requires complete wetting by the lubricant. In the manufacturing of photographic films, adhesion of the gelatin emulsions to the polymeric film base is vital. In xerography, the interaction of colloidal particles—polymer beads, toner particles—with surfaces determines the quality of the final print. In such applications, the interface is typically irregular, and the control of structure, chemical functionality, and roughness at the molecular level is practically impossible. As a result, the ability to modify surfaces in a predictable way and study their interfacial properties has been limited. Using SAMs allows for the systematic modification of surface free energy and chemical properties. The trapping of polymer chains near a surface,[269] and its dependence on surface functionalities can be investigated. The appearance of slippage at the wall depends on the polymer−wall interaction strength,[270] can also be studied.

Silberzan and Leger[271] and Novotny[272] measured the spreading rate of a polymer droplet on a surface and found that the measured diffusion constant was at least 1 order of magnitude smaller than that of the bulk. Recently, Zheng *et al.* measured the monomer−surface friction coefficient for polystyrene on a number of surfaces and obtained excellent agreement with reptation theory modified to account for increased friction due to surface−monomer contact.[273] By using molecularly engineered surfaces, a better understanding of the monomer−surface interaction mechanism can be achieved. Such understanding is key to understanding polymer behavior near surfaces, which has relevance to practical problems of wetting, coating, and adhesion. By using smooth, chemically homogeneous surfaces, and changing surface free energy in a systematic way, the contribution of chemistry to the polymer wetting mechanism can be addressed. When polymer properties (molecular weight and molecular weight distribution) are also altered systematically, the coupling between these two parameters can be investigated in detail.

Finally, engineered surfaces may contribute to the understanding of adhesion.[274] Control of adhesion is central to a large number of industrial processes and problems, but currently there is little if any understanding of how specific molecular ordering and interactions at the surface may affect adhesion.

Surfaces used in adhesion at the engineering level are far from being in a molecularly ordered well-characterized state. This makes it difficult to disentangle the relative importance of the many different effects that are ultimately responsible for adhesion. The complexity of adhesion phenomena may be addressed by minimizing the number of uncontrolled parameters, thus reducing the ambiguity. This can be accomplished by using SAMs as model surfaces.

V. References

(1) 1. Ulman, A. *An Introduction to Ultrathin Organic Films*; Academic Press: Boston, 1991.
(2) Bigelow, W. C.; Pickett, D. L.; Zisman, W. A. *J. Colloid Interface Sci.* **1946**, *1*, 513.
(3) Nuzzo, R. G.; Allara, D. L. *J. Am. Chem. Soc.* **1983**, *105*, 4481.
(4) Kuhn, H.; Ulman, A. In *Thin Films*; Ulman A., Ed.; Academic Press: New York, 1995; Vol. 20.
(5) Ball, P. *Designing the Molecular World*; Princeton University Press: Princeton, 1994.
(6) Ulman, A.; Evans, S. D.; Shnidman, Y.; Sharma, R.; Eilers, J. E.; Chang, J. C. *J. Am. Chem. Soc.* **1991**, *113*, 1499.
(7) Kumar, A.; Biebuyck, H. A.; Whitesides, G. M. *Langmuir* **1994**, *10*, 1498.
(8) Tirrell, D. A.; et al. *MRS Bull.* **1991**, July, 23−28.
(9) Allara, D. L.; Nuzzo, R. G. *Langmuir* **1985**, *1*, 45.
(10) Allara, D. L.; Nuzzo, R. G. *Langmuir* **1985**, *1*, 52.
(11) Ogawa, H.; Chihera, T.; Taya, K. *J. Am. Chem. Soc.* **1985** , *107*, 1365.
(12) Schlotter, N. E.; Porter, M. D.; Bright, T. B.; Allara, D. L. *Chem. Phys. Lett.* **1986**, *132*, 93.
(13) Huang, D. Y.; Tao, Y.-T. *Bull. Inst. Chem., Acad. Sin.* **1986**, *33*, 73.
(14) Shnidman, Y.; Ulman, A.; Eilers, J. E. *Langmuir* **1993**, *9*, 1071.
(15) Samart, M. G.; Brown, C. A.; Gordon, J. G. *Langmuir* **1993**, *9*, 1082.
(16) Tao, Y.-T. *J. Am. Chem. Soc.* **1993**, *115*, 4350.
(17) Thompson, W. R.; Pemberton, J. E. *Langmuir* **1995**, *11*, 1720.
(18) Smith, E. L.; Porter, M. D. *J. Phys. Chem.* **1993**, *97*, 4421.
(19) Soundag, A. H. M.; Tol, A. J. W.; Touwslager, F. J. *Langmuir* **1992**, *8*, 1127.
(20) Tao, Y.-T.; Lee, M.-T.; Chang, S.-C. *J. Am. Chem. Soc.* **1993**, *115*, 9547.
(21) Sagiv, J. *J. Am. Chem. Soc.* **1980**, *102*, 92.
(22) Silberzan, P.; Léger, L.; Ausserré, D.; Benattar, J. J. *Langmuir* **1991**, *7*, 1647.
(23) Wasserman, S. R.; Tao, Y. -T.; Whitesides, J. M. *Langmuir* **1989**, *5*, 1074.
(24) Le Grange, J. D.; Markham, J. L.; Kurjian, C. R. *Langmuir* **1993**, *9*, 1749.
(25) Maoz, R.; Sagiv, J. *J. Colloid Interface Sci.* **1984**, *100*, 465.
(26) Gun, J.; Sagiv, J. *J. Colloid Interface Sci.* **1986**, *112*, 457.
(27) Gun, J.; Iscovici, R.; Sagiv, J. *J. Colloid Interface Sci.* **1984**, *101*, 201.
(28) Tillman, N.; Ulman, A.; Schildkraut, J. S.; Penner, T. L. *J. Am. Chem. Soc.* **1988**, *110*, 6136.
(29) Brandriss, S.; Margel, S. *Langmuir* **1993**, *9*, 1232.
(30) Mathauser, K.; Frank, C. W. *Langmuir* **1993**, *9*, 3002.
(31) Mathauser, K.; Frank, C. W. *Langmuir* **1993**, *9*, 3446.
(32) Carson, G.;Granick, S. *J. Appl. Polym. Sci.* **1989**, *37*, 2767.
(33) Kessel, C. R.; Granick, S. *Langmuir* **1991**, *7*, 532.
(34) Schwartz, D. K.; Steinberg, S.; Israelachvili, J.; Zasadzinski, Z. A. N. *Phys. Rev. Lett.* **1992**, *69*, 3354.
(35) Finklea, H. O.; Robinson, L. R.; Blackburn, A.; Richter, B.; Allara, D. L.; Bright, T. *Langmuir* **1986**, *2*, 239.
(36) Rubinstein, I.; Sabatani, E.; Maoz, R.; Sagiv, J. *Proc. Electrochem. Soc.* **1986**, *86*, 175.
(37) Rubinstein, I.; Sabatani, E.; Maoz, R.; Sagiv, J. *Electroanal. Chem.* **1987**, *219*, 365.
(38) Allara, D. L.; Parikh, A. N.; Rondelez, F. *Langmuir* **1995**, *11*, 2357.
(39) Tripp, C. P.; Hair, M. L. *Langmuir* **1992**, *8*, 1120.
(40) Angst, D. L.; Simmons, G. W. *Langmuir* **1991**, *7*, 2236.
(41) McGovern, M. E.; Kallury, K. M. R.; Thompson, M. *Langmuir* **1994**, *10*, 3607.
(42) Wasserman, S. R.; Whitesides, G. M.; Tidswell, I. M.; Ocko, B. M; Pershan, P. S.; Axe, J. D. *J. Am. Chem. Soc.* **1989**, *111*, 5852.
(43) Tripp, C. P.; Hair, M. L. *Langmuir* **1995**, *11*, 149.
(44) Gao, W.; Reven, L. *Langmuir* **1995**, *11*, 1860.
(45) Bierbaum, K.; Kinzler, M.; Wöll, Ch.; Grunze, M.; Hähner, G.; Heid, S.; Effecberger, F. *Langmuir* **1995**, *11*, 512.
(46) Banga, R.; Yarwood, J.; Morgan, A. M.; Evans, B.; Kells, J. *Langmuir* **1995**, *11*, 4393.
(47) Cohen, S. R.; Naaman, R.; Sagiv, J. *J. Chem. Phys.* **1986**, *90*, 3054.
(48) Ohtake, T.; Mino, N.; Ogawa, K. *Langmuir* **1992**, *8*, 2081.
(49) Tidswell, I. M.; Ocko, B. M.; Pershan, P. S.; Wasserman, S. R.; Whitesides, G. M.; Axe, J. D. *Phys. Rev.* **1990**, *B 41*, 1111.
(50) Nakagawa, T.; Ogawa, K. *Langmuir* **1994**, *10*, 367.
(51) Okusa, H.; Kurihara, K.; Kunitake, T. *Langmuir* **1994**, *10*, 8.
(52) Fujii, M.; Sugisawa, S.; Fukada, K.; Kato, T.; Shirakawa, Y. T.; Seimiya, T. *Langmuir* **1994**, *10*, 984.
(53) Yoshino, N. *Chem. Lett.* **1994,** 735.
(54) Bierbaum, K.; Grunze, M. *Adhes. Soc.* **1994**, 213.
(55) Flinn, D. H.; Guzonas, D. A.; Yoon, R. -H. *Colloids Surf. A.* **1994**, *87*, 163.
(56) Rabinovich, Y.-I.; Yoon, R.-H. *Langmuir* **1994**, *10*, 1903.
(57) Siedlecki, C. A.; Eppell, S. LJ.; Marchant, R. E. *J. Biomed. Mater. Res.* **1994**, *28*, 271.
(58) Mathauer, K.; Frank, C. *Langmuir* **1993**, *9*, 3446.
(59) Netzer, L.; Iscovichi, R.; Sagiv, J. *Thin Solid Films* **1983**, *100*, 67.
(60) Pomerantz, M.; Segmüller, A.; Netzer, L.; Sagiv, J. *Thin Solid Films* **1985**, *132*, 153.
(61) Tillman, N.; Ulman, A.; Penner, T. L. *Langmuir* **1989**, *5*, 101.
(62) Kurth, D. G.; Bein, T. *Langmuir* **1993**, *9*, 2965.
(63) Kurth, D. G.; Bein, T. *Langmuir* **1995**, *11*, 3061.
(64) Durfor, C. N.; Turner, D. C.; Georger, J. H.; Peek, B. M.; Stenger, A. D. A. *Langmuir* **1994**, *10*, 148.
(65) Rühe, J.; Novotny, V. J.; Kanazawa, K. K.; Clarke, T.; Street, G. B. *Langmuir* **1993**, *9*, 2383.
(66) Xiao, X.-D.; Liu, G.-Y.; Charych, D. H.; Salmeron, M. *Langmuir* **1995**, *11*, 1600.
(67) Xiao, X.-D.; Hue, J.; Charych, D. H.; Salmeron, M. *Langmuir* **1996**, *12*, 235.
(68) Chaudhury, M. K.; Whitesides, G. M. *Science* **1992**, *255*, 1230.
(69) Balachander, N.; Sukenik, C. N. *Langmuir* **1990**, *6*, 1621.
(70) Lee, Y. W.; Reed-Mundell, J.; Sukenik, C. N.; Zull, J. E. *Langmuir* **1993**, *9*, 3009.
(71) Chupa, J. A.; Xu, S.; Fishchetti, R. F.; Strongin, R. M.; McCauley, J. P.; Smith, A. B.; Blasie, J. K. *J. Am. Chem. Soc.* **1993**, *115*, 4383.
(72) Paulson, S.; Morris, K.; Sullivan, B. P. *J. Chem. Soc., Chem. Commun.* **1992**, 1615.
(73) Wasserman, S. R.; Biebuyck, H.; Whitesides, G. M. *J. Mater. Res.* **1989**, *4*, 886.
(74) Maoz, M.; Sagiv, J. *Langmuir* **1987**, *3*, 1034.
(75) Maoz, M.; Sagiv, J. *Langmuir* **1987**, *3*, 1045.
(76) Maoz, R.; Netzer, L.; Gun, J.; Sagive, J. *J. Chim. Phys. (Paris)* **1988**, *85*, 1059.
(77) Netzer, L.; Iscovici, R.; Sagiv, J. *Thin Solid Films* **1983**, *99*, 235.
(78) Netzer, R.; Sagiv, J. *J. Am. Chem. Soc.* **1983**, *105*, 674.
(79) Maoz, R.; Sagiv, J. *Thin Solid Films* **1985**, *132*, 135.
(80) Ogawa, K.; Mino, N.; Tamura, H.; Hatada, M. *Langmuir* **1990**, *6*, 851.
(81) Ogawa, K.; Mino, N.; Tamura, H.; Hatada, M. *Langmuir* **1990**, *6*, 1807.
(82) Li, D. Q.; Ratner, M. A.; Marks, T. J.; Zhang, C. H.; Yang, J.; Wong, G. K. *J. Am. Chem. Soc.* **1990**, *112*, 7389.
(83) Kakkar, A. K.; Yitzchaik, S.; Roscoe, S. B.; Kubota, F.; Allan, D. S.; Marks, T. J.; Xu, Z.; Lin, W.; Wong, G. K. *Langmuir* **1993**, *9*, 388.
(84) Yitzchaik, S.; Roscoe, S. B.; Kakkar, A. K.; Allan, D. S.; Marks, T. J.; Xu, Z.; Zhang, T.; Lin, W.; Wong, G. K. *J. Phys. Chem.* **1993**, *97*, 6958.
(85) Roscoe, S. B.; Yitzchaik, S.; Kakkar, A. K.; Marks, T. J.; Lin, W. L.; Wong, G. K. *Langmuir* **1994**, *10*, 1337.
(86) Wegner, G. *Thin Solid Films* **1992**, *216*, 105.
(87) Tripp, C. P.; Veregin, R. P. N.; Hair, M. L. *Langmuir* **1993**, *9*, 3518.
(88) Jeon, L. J.; Nuzzo, R. G.; Xia, Y.; Mrksich, M.; Whitesides, G. M. *Langmuir* **1995**, *11*, 3024.
(89) Xia, Y.; Mrksich, M.; Kim, E.; Whitesides, G. M. *J. Am. Chem. Soc.* **1995**, *117*, 9576.
(90) Dressick, W. J.; Dulcey, C. S.; Georger, J. H.; Calvert, J. M. *Chem. Mater.* **1993**, *5*, 148.
(91) Chen, K.; Caldwell, W. B.; Mirkin, C. A. *J. Am. Chem. Soc.* **1993**, *115*, 1193.
(92) Li, D. Q.; Swanson, B. I. *Langmuir* **1993**, *9*, 3341.
(93) Tsukruk, V. V.; Lander, L. M.; Brittain, W. L. *Langmuir* **1994**, *10*, 996.
(94) Hong, H.-H.; Jiang, M.; Slinger, S. G.; Bohn, P. *Langmuir* **1994**, *10*, 153.
(95) Offord, D. A.; Griffin, J. H. *Langmuir* **1993**, *9*, 3015.
(96) Sukenik, C. N. Private communication.
(97) Robinson, K.; Ulman, A.; Lando, J.; Mann, A. J. Unpublished results.

(98) Lin, W.; Yitzchaik, S.; Lin, W.; Malik, A.; Durbin, M. K.; Richter, A. G.; Wong, G. K.; Dutta, P.; Marks, T. *Angew. Chem., Int. Ed. Engl.* **1995**, *34*, 1497.
(99) Maoz, R.; Yam, R.; Berkovic, G.; Sagiv, J. In *Thin Films*; Ulman A., Ed.; Academic Press: New York, 1995; Vol. 20.
(100) Maoz, R.; Sagiv, J.; Degenhardt, D.; Möhwald, H.; Quint, P. *Supramol. Sci.* **1995**, *2*, 9.
(101) Mino, N.; Ogawa, K.; Hatada, M.; Takastuka, M.; Sha, S.; Moriizumi, T. *Langmuir* **1993**, *9*, 1280.
(102) Mino, N.; Ogawa, K.; Hatada, M.; Takatsuka, M.; Sha, S.; Morizumi, T. *Langmuir* **1993**, *9*, 1280.
(103) Dubois, L. H.; Nuzzo, R. G. *Ann. Phys. Chem.* **1992**, *43*, 437.
(104) Bain, C. D.; Whitesides, G. M. *Adv. Mater.* **1989**, *1*, 506.
(105) Folkers, J. P.; Zerkowski, J. A.; Laibinis, P. E.; Seto, C. T.; Whitesides, G. M. *Supramolecular architecture*; Bein, T. Ed.; ACS Symposium Series 499; American Chemical Society: Washington, DC, 1992; pp 10−23.
(106) Lee, T. R.; Laibinis, P. E.; Folkers, J. P.; Whitesides, G. M. *Pure Appl. Chem.* **1991**, *63*, 821.
(107) Whitesides, G. M.; Ferguson, G. S. *Chemtracts-Org. Chem.* **1988**, *1*, 171.
(108) Sellers, H.; Ulman, A.; Shnidman, Y.; Eilers, J. E. *J. Am. Chem. Soc.* **1993**, *115*, 9389.
(109) Troughton, E. B.; Bain, C. D.; Whitesides, G. M.; Allara, D. L.; Porter, M. D. *Langmuir* **1988**, *4*, 365.
(110) Katz, E.; Itzhak, N.; Willner, I. *J. Electroanal. Chem.* **1992**, *336*, 357.
(111) Sabatani, E.; Cohen-Boulakia, J.; Bruening, M.; Rubinstein, I. *Langmuir* **1993**, *9*, 2974.
(112) Bryant, M. A.; Joa, S. L.; Pemberton, J. E. *Langmuir* **1992**, *9*, 753.
(113) Hill, W.; Wehling, B. *J. Phys. Chem.* **1993**, *97*, 9451.
(114) Li, T. T.-T.; Liu, H. Y.; Weaver, M. J. *J. Am. Chem. Soc.* **1984**, *106*, 1233.
(115) Cooper, J. M.; Greenough, K. R.; McNeil, C. J. *J. Electroanal. Chem.* **1993**, *347*, 267.
(116) Uvdal, K.; Bodö, P.; Liedberg, B. *J. Colloid Interf. Sci.* **1992**, *149*, 162.
(117) Ihs, A.; Uvdal, K.; Liedberg, B. *Langmuir* **1993**, *9*, 733.
(118) Arndt, Th.; Schupp, H.; Schepp, W. *Thin Solid Films* **1989**, *178*, 319.
(119) Mielczarski, J. A.; Yoon, R. H. *Langmuir* **1991**, *7*, 101.
(120) Edwards, T. R. G.; Cunnane, V. J.; Parsons, R.; Gani, D. *J. Chem. Soc., Chem. Commun.* **1989**, 1041.
(121) Arduengo, A. J.; Moran, J. R.; Rodriguez-Paradu, J.; Ward, M. D. *J. Am. Chem. Soc.* **1990**, *112*, 6153.
(122) Xue, G.; Huang, X.-Y.; Dong, J.; Zhang, J. *J. Electroanal. Chem.* **1991**, *310*, 139.
(123) Bharathi, S.; Yegnaraman, V.; Rao, G. P. *Langmuir* **1993**, *9*, 1614.
(124) Samanat, M. G.; Broen, C. A.; Gordon, J. G. *Langmuir* **1992**, *8*, 1615.
(125) Somorjai, G. A. *Chemistry in Two Dimensions - Surfaces*; Cornell University Press: Ithaca, New York, 1982.
(126) King, D. E. *J. Vac. Sci. Technol.* **1995**, in press.
(127) Ulman, A. *J. Mater. Educ.* **1989**, *11*, 205.
(128) Laibinis, P. E.; Whitesides, G. M.; Allara, D. L.; Tao, Y. -T.; Parikh, A. N.; Nuzzo, R. G. *J. Am. Chem. Soc.* **1991**, *113*, 7152.
(129) Walczak, M. W.; Chung, C.; Stole, S. M.; Widrig, C. A.; Porter, M. D. *J. Am. Chem. Soc.* **1991**, *113*, 2370.
(130) Laibinis, P. E.; Whitesides, G. M. *J. Am. Chem. Soc.* **1992**, *112*, 1990.
(131) Ihs, A.; Liedberg, B. *Langmuir* **1994**, *10*, 734.
(132) Laibinis, P. E.; Whitesides, G. M. *J. Am. Chem. Soc.* **1992**, *114*, 9022.
(133) Shimazu, K.; Sato, Y.; Yagi, I.; Uosaki, K. *Bull. Chem. Soc. Jpn.* **1994**, *67*, 863.
(134) Demoz, A.; Harrison, D. J. *Langmuir* **1993**, *9*, 1046.
(135) Muskal, N.; Turyan, I.; Shurky, A.; Mandler, D. *J. Am. Chem. Soc.* **1995**, *117*, 1147. .
(136) Stratmann, M. *Adv. Mater.* **1990**, *2*, 191.
(137) Volmer, M.; Stratmann, M.; Viefhaus, H. *Surf. Interface Anal.* **1990**, *16*, 278.
(138) Liu, Q.; Xu, Z. *Langmuir* **1995**, *11*, 4617.
(139) Brust, M.; Walker, M.; Bethell, D.; Schiffrin, D. J.; Whyman, R. *J. Chem. Soc., Chem. Commun.* **1994**, 801.
(140) Sheen, C. W.; Shi, J. X.; Martensson, J.; Parikh, A. N.; Allara, D. L. *J. Am. Chem. Soc.* **1992**, *114*, 1514.
(141) Gu, Y.; Lin, B.; Smentkowski, V. S.; Waldeck, D. H. *Langmuir* **1995**, *11*, 1849.
(142) Ulman, A. Unpublished results.
(143) Bain, C. D.; Troughton, E. B.; Tao, Y.-T.; Evall, J.; Whitesides, G. M.; Nuzzo, R. G. *J. Am. Chem. Soc.* **1989**, *111*, 321.
(144) Buck, M.; Eisert, F.; Fischer, J.; Grunze, M.; Träger, F. *Appl. Phys.* **1991**, *A53*, 552.
(145) Buck, M.; Eisert, F.; Grunze, M. *Ber. Bunsen-Ges. Phys. Chem.* **1993**, *97*, 399.
(146) Hähner, G.; Wöll, Ch.; Buck, M.; Grunze, M. *Langmuir* **1993**, *9*, 1955.
(147) Evans, S. D.; Urankar, E.; Ulman, A.; Ferris N. *J. Am. Chem. Soc.* **1991**, *113*, 4121.
(148) Offord, D. A.; John, C. M.; Linford, M. R.; Griffin, J. H. *Langmuir* **1994**, *10*, 883.
(149) Biebuyck, H. A.; Bain, C. D.; Whitesides, G. M. *Langmuir* **1994**, *10*, 1825.
(150) Biebuyck, H. A.; Whitesides, G. M. *Langmuir* **1993**, *9*, 1766.
(151) Mohri, N.; Inoue, M.; Arai, Y.; Yoshikawa, K. *Langmuir* **1995**, *11*, 1612.
(152) Fenter, P.; Eberhardt, A.; Eisenberger, P. *Science* **1994**, *266*, 1216.
(153) Thomas, R. C.; Sun, L.; Crooks, M. *Langmuir* **1991**, *7*, 620.
(154) Chailapakul, O.; Sun, L.; Xu, C.; Crooks, M. *J. Am. Chem. Soc.* **1993**, *115*, 12459.
(155) Porter, M. D.; Bright, T. B.; Allara, D. L.; Chidsey, C. E. D. *J. Am. Chem. Soc.* **1987**, *109*, 3559.
(156) Nuzzo, R. G.; Fusco, F. A.; Allara, D. L. *J. Am. Chem. Soc.* **1987**, *109*, 2358.
(157) Bain, C. D.; Biebuyck, H. A.; Whitesides, G. M. *Langmuir* **1989**, *5*, 723.
(158) Nuzzo, R. G.; Zegarski, B. R.; Dubois, L. H. *J. Am. Chem. Soc.* **1987**, *109*, 733.
(159) Nuzzo, R. G.; Dubois, L. H.; Allara, D. L. *J. Am. Chem. Soc.* **1990**, *112*, 558.
(160) Li, Y.; Huang, J.; McIver, R. T., Jr.; Hemminger, J. C. *J. Am. Chem. Soc.* **1992**, *114*, 2428.
(161) Widrig, C. A.; Chung, C.; Porter, M. D. *J. Electroanal. Chem.* **1991**, *310*, 335.
(162) Bryant, M. A.; Pemberton, J. E. *J. Am. Chem. Soc.* **1991**, *113*, 3630; **1991**, *113*, 8284.
(163) Bryant, M. A.; Pemberton, J. E. *J. Am. Chem. Soc.* **1991**, *113*, 8284.
(164) Schlenoff, J. B.; Li, M.; Ly, H. *J. Am. Chem. Soc.* **1995**, *117*, 12528.
(165) Hickman, J. J.; Ofer, D.; Zou, C.; Wrighton, M. S.; Laibinis, P. E.; Whitesides, G. M. *J. Am. Chem. Soc.* **1991**, *113*, 1128.
(166) Collard, D. M.; Fox, M. A. *Langmuir* **1991**, *7*, 1192.
(167) Groat, K. A.; Creager, S. E. *Langmuir* **1993**, *9*, 3668.
(168) Ravenscroft, M. S.; Finklea, H. O. *J. Phys. Chem.* **1994**, *98*, 3843.
(169) Curtin, L. S.; Peck, S. R.; Tender, L. M.; Murray, R. W.; Rowe, G. K.; Creager, S. E. *Anal. Chem.* **1993**, *65*, 368.
(170) Zhong, C. J.; Porter, M. D. *J. Am. Chem. Soc.* **1994**, *116*, 11616.
(171) Jaffey, D. M.; Madix, R. J. *J. Am. Chem. Soc.* **1994**, *116*, 3012.
(172) Strong, L.; Whitesides, G. M. *Langmuir* **1988**, *4*, 546.
(173) Chidsey, C. E. D.; Loiacono, D. N. *Langmuir* **1990**, *6*, 709.
(174) Dubois, L. H.; Zegarski, B. R.; Nuzzo, R. G.; *J. Chem. Phys.* **1993**, *98*, 678.
(175) Chidsey, C. E. D.; Liu, G.-Y.; Rowntree, Y. P.; Scoles, G. *J. Chem. Phys.* **1989**, *91*, 4421.
(176) Alves, C. A.; Smith, E. L.; Porter, M. D. *J. Am. Chem. Soc.* **1992**, *114*, 1222.
(177) Poirier, G. E.; Tarlov, M. J.; Rushneier, H. E.; *Langmuir* **1994**, *10*, 3383.
(178) Fenter, P.; Eisenberger, P.; Liang, K. S. *Phys. Rev. Lett.* **1993**, *70*, 2447.
(179) Camillone, N.; Chidsey, C. E. D.; Liu, G.-Y.; Scoles, G. *J. Phys. Chem.* **1993**, *98*, 3503.
(180) Poirier, G. E; Tarlov, M. J. *Langmuir* **1994**, *10*, 2859.
(181) Edinger, G.; Gölzhäuser, A.; Demota, K.; Wöll, Ch.; Grunze, M. *Langmuir* **1993**, *9*, 4.
(182) Schönenberger, C.; Sondag-Huethorst, J. A. M.; Jorritsma, J.; Fokkink, L. G. J. *Langmuir* **1994**, *10*, 611.
(183) Sellers, H. *Surf. Sci.* **1993**, *294*, 99.
(184) Grunze, M. *Phys. Scr.* **1993**, in press.
(185) McCarley, R. L.; Dunaway, D. J.; Willicut, R. J. *Langmuir* **1993**, *9*, 2775.
(186) Bucher, J. -P.; Santesson, L.; Kern, K. *Langmuir* **1994**, *10*, 979.
(187) Scoles, G. Private communication.
(188) Schwaha, K.; Spencer, N. D.; Lambert, R. M. *Surf. Sci.* **1979**, *81*, 273.
(189) Rovida, G.; Pratesi, F. *Surf. Sci.* **1981**, *104*, 609.
(190) Harris, A. L.; Chidsey, C. E. D.; Levinos, N. J.; Loiacono, D. N. *Chem. Phys. Lett.* **1987**, *141*, 350.
(191) Harris, A. L.; Rothberg, L.; Dhar, L.; Levinos, N. J.; Dubois, L. H. *J. Phys. Chem.* **1991**, *94*, 2438.
(192) Seto, T.; Hara, T.; Tanaka, K. *Jpn. J. Appl. Phys.* **1968**, *7*, 31.
(193) Fenter, P.; Eisenberger, P.; Li, J.; Chamillone, N.; Bernasek, S.; Scoles, G.; Ramanarayanan, T. A.; Liang, K. S. *Langmuir* **1991**, *7*, 2013.
(194) Dhirani, A.; Hines, M. A.; Fisher, A. J.; Ismail, O.; Guyot-Sionnest, P. *Langmuir* **1995**, *11*, 2609.
(195) Ulman, A.; Eilers, J. E.; Tillman, N. *Langmuir* **1989**, *5*, 1147.
(196) Gui, J. Y.; Stern, D. A.; Frank, D. G.; Lu, F.; Zapien, D. C.; Hubbard, A. T. *Langmuir* **1991**, *7*, 955.
(197) Gui, J. Y; Lu, F.; Stern, D. A.; Hubbard, A. T. *J. Electroanal. Chem.* **1990**, *292*, 245.
(198) Nemetz, A.; Fischer, T.; Ulman, A.; Knoll, W. *J. Chem. Phys.* **1993**, *98*, 5912.
(199) Fenter, P.; Eisenberger, P. Private communication.
(200) Chidsey, C. E. D.; Loiacono, D. N. *Langmuir* **1990**, *6*, 682.
(201) Dohlhofer, K.; Figura, J.; Fuhrhop, J.-H. *Langmuir* **1992**, *8*, 1811.
(202) Chidsey, C. E. D.; Bertozzi, C. R.; Putvinski, T. M.; Mujsce, A. M. *J. Am. Chem. Soc.* **1990**, *112*, 4301.

(203) Uosaki, K.; Sato, Y.; Kita, H. *Langmuir* **1991**, *7*, 1510.
(204) Chidsey, C. E. D. *Science* **1991**, *251*, 919.
(205) Popenoe, D. D.; Deinhammer, R. S.; Porter, M. D. *Langmuir* **1992**, *8*, 2521.
(206) Sato, Y.; Frey, B. L.; Corn, R. M.; Uosaki, K. *Bull. Chem. Soc. Jpn.* **1994** ,*67*, 21.
(207) Creager, S. E.; Rowe, G. K. *Anal. Chim.* **1991**, *246*, 233.
(208) Rowe, G. K.; Creager, S. E. *Langmuir* **1991**, *7*, 2307.
(209) Rowe, G. K.; Creager, S. E. *Langmuir* **1994**, *10*, 1186.
(210) Häussling, L.; Ringsdorf, H.; Schmitt, F.-J.; Knoll, W. *Langmuir* **1991**, *7*, 1837.
(211) Häussling, L.; Michel, B.; Ringsdorf, H.; Rohrer, H. *Angew. Chem., Int. Ed. Engl.* **1991**, *30*, 679.
(212) Schmitt, F.-J.; Häussling, L.; Ringsdorf, H.; Knoll, W. *Thin Solid Films* **1992**, *210/211*, 815.
(213) Spinke, J.; Liley, J.; Guder, H.-J.; Angermaier, L.; Knoll, W. *Langmuir* **1993**, *9*, 1821.
(214) Spinke, J.; Liley, M.; Schmitt, F.-J.; Guder, H.-J.; Angermaier, L.; Knoll, W. *J. Chem. Phys.* **1993**, *99*, 7012.
(215) Obeng, Y. S.; Bard, A. J. *Langmuir* **1991**, *7*, 195.
(216) Yip, C. M.; Ward, M. D. *Langmuir* **1994**, *10*, 549.
(217) Zak, J.; Yuan, H.; Woo, K.; Porter, M. D. *Langmuir* **1993**, *9*, 2772.
(218) Hutchinson, J. E.; Postlethwaite, T. A.; Murray, R. W. *Langmuir* **1993**, *9*, 3277.
(219) Herr, B. R.; Mirkin, C. A. *J. Am. Chem. Soc.* **1994**, *116*, 1157.
(220) Sun, L.; Kepley, J.; Crooks, R. M. *Langmuir* **1992**, *8*, 2101.
(221) Sun, L.; Crooks, R. M.; Ricco, A. J. *Langmuir* **1993**, *9*, 1775.
(222) Duevel, R. V.; Corn, R. M. *Anal. Chem.* **1992**, *64*, 337.
(223) Kim, T.; Crooks, R. M.; Tsen, M.; Sun, L. Preprint.
(224) Ulman, A.; Tillman, N. *Langmuir* **1989**, *5*, 1418.
(225) Sun, L.; Thomas, R. C.; Crooks, R. M.; Ricco, A. J. *J. Am. Chem. Soc.* **1991**, *113*, 8550.
(226) Xu, C.; Sun, L.; Kepley, L. J.; Crooks, R. M. *Anal. Chem.* **1993**, *65*, 2102.
(227) Schilling, M. L.; Katz, H. E.; Stein, S. M.; Shane, S. F.; Wilson, W. L.; Buratto, S.; Ungahse, S. B.; Taylor, G. N.; Putvinski, T. M.; Chidsey, C. E. D. *Langmuir* **1993**, *9*, 2156.
(228) Bent, S. F.; Schilling, M. L.; Wilson, W. L.; Katz, H. E.; Harris, A. L. *Chem. Mater.* **1994**, *6*, 122.
(229) Bertilsson, L.; Liedberg, B. *Langmuir* **1993**, *9*, 141.
(230) Evans, S. D.; Sharma, R; Ulman, A. *Langmuir* **1991**, *7*, 156.
(231) Löfås, S.; Johnsson, B. *J. Chem. Soc., Chem. Commun.* **1990**, 1526.
(232) Wilner, I.; Riklin, A.; Shoham, B.; Rivenson, D.; Katz, E. *Adv. Mater.* **1993**, *5*, 912.
(233) Keller, H.; Schrepp, W.; Fuchs, H. *Thin Solid Films* **1992**, *210/211*, 799.
(234) Linford, M. R.; Chidsey, C. E. D. *J. Am. Chem. Soc.* **1993**, *115*, 12631.
(235) Linford, M. R.; Chidsey, C. E. D.; Fenter, P.; Eisenberger, P. M. *J. Am. Chem. Soc.* **1995**, *116*, in press.
(236) Cao, G.; Hong, H.-G.; Mallouk, T. E. *Acc. Chem. Res.* **1992**, *25*, 420.
(237) Lee, H.; Kepley, L. J.; Hong, H.-G.; Mallouk, T. E. *J. Am. Chem. Soc.* **1988**, *110*, 618.
(238) Lee, H.; Kepley, L. J.; Hong, H.-G.; Akhter, S.; Mallouk, T. E. *J. Phys. Chem.* **1988**, *92*, 2597.
(239) Katz, H. E.; Schilling, M. L.; Ungahse, S. B.; Putvinski, T. M.; Chidsey, C. E. D. *Supramolecular Architecture*; Bein, T., Ed.; ACS Symposium Series 499; American Chemical Society: Washington, DC, 1992; pp 24−32.
(240) Katz, H. E.; Schilling, M. L.; Chidsey, C. E. D.; Putvinski, T. M.; Hutton, R. S. *Chem. Mater.* **1991**, *3*, 699.
(241) Ungahse, S. B.; Wilson, W. L.; Katz, H. E.; Scheller, R. G.; Putvinski, T. M. *J. Am. Chem. Soc.* **1992**, *114*, 8717.
(242) Putvinski, T. M.; Schilling, M. L.; Katz, H. E.; Chidsey, C. E. D.; Mujsce, A. M.; Emerson, A. B. *Langmuir* **1990**, *6*, 1567.
(243) Katz, H. E.; Scheller, R. G.; Putvinski, T. M.; Schilling, M. L.; Wilson, W. L.; Chidsey, C. E. D. *Science* **1991**, *254*, 1485.
(244) Katz, H. E.; Schilling, M. L. *Chem. Mater.* **1993**, *5*, 1162.
(245) Outka, D. A.; Stöhr, J.; Rabe, J. P.; Swalen, J. D.; Rotermund, H. H. *Phys. Rev. Lett.* **1987**, *59*, 1321.
(246) Ulman, A.; Scaringe, R. P. *Langmuir* **1992**, *8*, 894.
(247) Scaringe, R. P. In *Electron Crystallography of Organic Molecules*; Fryer, J. R., Dorset, D. L., Eds.; Kluwer: Dordrecht, 1990; pp 85−113.
(248) Camillone, N.; Chidsey, C. E. D.; Liu, G.-Y.; Scoles, G. *J. Chem. Phys.* **1993**, *98*, 4234.
(249) Eilers, J. E. Unpublished results.
(250) Evans, S. D.; Goppert-Berarducci, K.; Urankar, E.; Gerenser, L. J.; Ulman, A. *Langmuir* **1991**, *7*, 2700.
(251) Tam-Chang, S.-W.; Biebuyck, H. A.; Whitesides, G. M.; Jeon, N.; Nuzzo, R. G. *Langmuir* **1995**, *11*, 4371.
(252) Allara, D. L. In *Polymer Surfaces and Interfaces*; Feast, W. J., Munro, H. S., Richards, R. W., Eds.; Wiley: Chichester, 1993; Vol. II, p 27.
(253) Finklea, H. O.; Hanshew, D. D. *J. Am. Chem. Soc.* **1992**, *114*, 3173.
(254) Finklea, H. O.; Hanshew, D. D. *J. Electroanal. Chem.* **1993**, *347*, 327.
(255) Olbris, J. O.; Ulman, A.; Shnidman, Y. *J. Chem. Phys.* **1995**, *102*, 6865.
(256) Hautman, J.; Klein, M. L. *Phys. Rev. Lett.* **1991**, *67*, 1763.
(257) Hautman, J.; Bareman, J. P.; Mar, W.; Klein, M. L. *J. Chem. Soc., Faraday Trans.* **1991**, *87*, 2031.
(258) Potochnik, S. J.; Pehrsson, P. E.; Hsu, D. S. Y.; Calvert, J. M. *Langmuir* **1995**, *11*, 1842 and references therein.
(259) Kumar, A.; Abbott, N. L.; Kim, E.; Biebuyck, H. A.; Whitesides, G. M. *Acc. Chem. Res.* **1995**, *28*, 219.
(260) Mallouk, T. E., Harrison, D. J., Eds., *Interfacial Design and Chemical Sensing*; ACS Symposium Ser. 561; American Chemical Society: Washington, DC, 1994.
(261) Carron, K. T.; Pelterson, L.; Lewis, M. *Environ. Sci. Technol.* **1992**, *26*, 1950.
(262) Kepley, L. J.; Crooks, R. M.; Ricco, A. *J. Anal. Chem.* **1992**, *64*, 3191.
(263) Schierbaum, K. D.; Weiss, T.; Thoden van Velzen, J. F. J.; Reinhoudt, D. N.; Goepel, W. *Science* **1994**, *265*, 1413.
(264) Duan, C. M.; Meyerhoff, M. E. *Anal. Chem.* **1994**, *66*, 1369.
(265) Kajiya, Y.; Okamoto, T.; Yoneyama, H. *Chem. Lett.* **1993**, *12*, 2107.
(266) Chung, C.; Porter, M. D. *Chem. Eng. News* **1989**, May 1, 32.
(267) Rojas, M. T.; Koniger, R.; Stoddart, J. F.; Kaifer, A. E. *J. Am. Chem. Soc.* **1995**, *117*, 336.
(268) Steinberg, S.; Tor, Y.; Sabatani, E.; Rubinstein, I. *J. Am. Chem. Soc.* **1991**, *113*, 5176.
(269) deGennes, P. G. *Conference Proceedings Liquids at Interfaces*; Charvolin, J., Joanny, J. F., Zinn-Justin, J., Eds.; Les Houches 1998; North Holland: Amsterdam, 1990.
(270) Manias, E.; Hadziioannou, G.; Bitsanis, I.; ten Brinke, G. *Europhys. Lett.* **1996**, in press.
(271) Silberzan, P.; Leger, L. *Macromolecules* **1992**, *25*, 1267.
(272) Novotny, V. J. *J. Chem. Phys.* **1990**, 3189.
(273) Zheng, X.; Sauer, B. B.; Van Alsten, J. G.; Schwarz, S. A.; Rafailovich, M. H.; Sokolov, J.; Rubinstein, M. *Phys. Rev. Lett.* **1995**, *74*, 407.

CR9502357